**Andjelka N. Hedrih**[1]

## BIOLOGICAL OSCILLATORS

*Abstract.* There are many oscillatory processes within biological systems. The whole human body is a complex system of coupled and synchronized oscillators. The mode of coupling can be very different. Oscillatory processes exist at almost every scale in human body: from systems of organs to subcellular structures and molecules. Using knowledge from several scientific fields (biology, medicine, theory of oscillations, theory of elasticity, rheology, non-linear dynamics), a complex multidisciplinary methodology for studying a wide class of oscillatory biodynamic models has been set. The principle of phenomenological mapping has been used in developing each of the oscillatory models of biological oscillators. In this review, oscillatory models of three different structures will be presented: the oscillatory model of double DNA chain helix, oscillatory model of zona pellucida and conditions for successful fertilisation, and oscillatory model of the mitotic spindle. These models are based on oscillations of chain systems. The DNA double helix is considered as a molecular biological oscillator, mitotic spindle as a subcellular system of coupled oscillators, and zona pellucida as an oscillating spherical net of cross-chains of oscillators that envelopes the female reproductive cell – the oocyte, at the surface of which an interaction with male reproductive cell- spermatozoa occurs. Assumptions of mathematical oscillatory models are presented as well as conditions for resonance. Some numerical analysis are also presented.

*Mathematics Subject Classification* (2010): Primary: 70-99, 74-99, 70F35, 92C10, 74L10; Secondary: 70Exx, 70KXX, 74M05, 37H20.

*Keywords:* biological oscillators, zona pellucida, DNA double helix, mitotic spindle, free and forced oscillations.

[1] Mathematical Institute of Serbin Academy of Sciences and Arts,
Kneza Mihaila 36, 11 000 Belgrade, Serbia
handjelka@turing.mi.sanu.ac.rs

## Contents

# 1. Introduction

Biological systems of different scales of complexity can function as oscillators from the molecular level to the level of the system of organs. Fine tuning of their synchronous work is in their physical and functional way of coupling making it work like a symphony. Resonance in a mechanical system can increase the amplitudes of oscillations to infinity leading to breakage or cracks into the system that could be desirable or undesirable. The specific cracks in the system change structural properties of the system. Different structural properties may affect the function of the system to a certain level. All these events are possible in biological systems according to the phenomenological mapping theory. It is possible to transfer knowledge from one scientific field to another, and to use the same mathematical methodology to describe different biological or technical processes with equal assumptions. Some phenomena are universal and exist both in living and in artificially created systems.

In this review, different biological systems are modeled as oscillators. In modelling, we tried to preserve the structural organization of the biological system we modeled and to give some answers on how the system works as a biomechanical system. The theory of oscillations is the main theory that is used in these modeling. In this review, three different oscillatory models will be presented: an oscillatory model of a double DNA helix, an oscillatory spherical net model of mouse zona pelucida

and an oscillatory model of a mitotic spindle. Results of mathematical modeling of all these three biological oscillators brings new light into the understanding of their functions from a biomechanical point of view thus contributing to biochemical understanding of the process.

All three models were created as a result of original work on the project NO 174001 (project leader prof. dr Katica (Stevanovic) Hedrih) financially supported by the Ministry of education, sciences and technological developement of the Republic of Serbia through the Mathematical Institute of the Serbian Academy of Sciences and Arts (MI SANU).

## 2. Oscillatory model of double DNA chain helix

Summary. Oscillatory models of the DNA chain are a part of research related to the mathematical modeling of the system of DNA molecules as an oscillatory chain system. The papers considers the corresponding oscillatory modes in the free and forced mode of oscillation of DNA molecules, as well as the possibility of resonance and dynamic absorption under the conditions of forced oscillation corresponding to the transcription process. It has been mathematically shown that a double DNA strand can be separated into two independent chains that oscillate with a different set of natural circular frequencies that could correspond to a sequence of base pairs in the double strand of DNA in a living cell. According to the mathematical analytical expressions of the double-strand oscillatory model, for special cases when a single-frequency force acts on a DNA molecule in the general case, there are different cases of resonant states that can occur in a single DNA chain. It has been shown mathematically that there are no interactions between two chains in terms of energy transfer from one chain to another.

### 2.1. Mathematical models of a double DNA molecule. DNA molecule is a complex polymer that codes genetic information the dynamics of which were studied through many different approaches and biomechanical models (polymer models, elastic rod model, network model, torsional springs model, soliton-existence supporting models, multi-pendulum models) [1].

Stretching and twisting properties of DNA's were obtained through different techniques (optical tweezers, atomic force microscopy and single-molecule technique, dielectrophoresis) [2–4]. "Double-stranded DNA (dsDNA) expresses sequence-dependent flexibility on the sub-microsecond timescale. Pyrimidine-purine type steps are the most flexible, purine-purine steps are about average, and purine-pyrimidine steps are the most inflexible" (Okonogi et al., 2002 by [1]).

We propose a multi pendulum models of double DNA [5–8]. Models are based on DNA model by N. Kovaleva and L. Manevich [9, 10] and dynamics in chain systems [11]. The pendulum models differ in the way its elements (base pairs) are coupled, from pure elastic to hereditary properties: the model with elastic properties, model with fractional [7, 12, 13] and model with hereditary properties [8, 12]. In a pure elastic model, elements are interconnected with elastic springs, in the fractional

model with standard light fractional order creep elements and in the model with hereditary properties with standard light hereditary element. As DNA molecule ages [14] we suggest that DNA molecule might also be changing its mechanical properties during aging. In this light of dDNA aging phenomenon, different types of oscillatory models of dDNA were considered regarding the way of coupling the polymer elements of dDNA. Free and forced vibrations[7, 12], eigen modes [15] and the transfer of energy through double DNA [5] chains were analysed.

Constitutive stress-strain relation for the restitution force as the function of element elongation for standard light hereditary element is given by an integral member in the form:

$$P(t) = -c_0 \left[ x(t) - \int_0^t \Re(t-\tau)x(\tau)d\tau \right] = -c_0 \left[ x(t) - \Im[x(t)] \right] \qquad (1)$$

$\Re(t-\tau) = \dfrac{c_\sigma - c_0}{nc_\sigma} e^{-\frac{1}{n}(t-\tau)}$ is relaxation kernel $\beta = \dfrac{1}{n}$ is coefficient of the element relaxation.

Different boundary conditions of the double DNA chain helix were taken into account: the cases when the ends of chains are either free or fixed. Fig. 1. and Fig 2.



FIGURE 1. Multi-pendulum model of dDNA helix with free ends. Example of Ideally elastic model. Taken from [15].
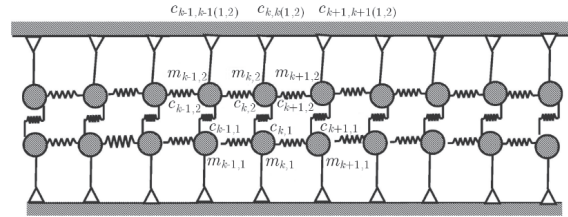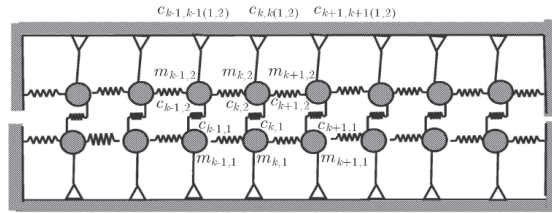


FIGURE 2. Multi-pendulum model of dDNA helix with fixed ends. Example of Ideally elastic model. Taken from [15].

In each of the models (ideally elastic, fractional and hereditary), the complex methodology was derived to generate the generalized and main coordinates of each base pair in the chains system. Mathematically, it is possible to obtain two fictive

decoupled and separated single eigen chains of the double DNA helix, a different set of eigen circular frequencies of decupled dDNA helix in all type of oscillatory dDNA models. "This may correspond to different chemical structure (the order of base pairs) of the complementary chains of DNA. We are free to propose that every specific set of the base pair order has its circular eigen frequencies, and it changes when DNA chains are coupled in the system of double helix"[6].

The models are suitable for studying resonance phenomena and phenomena of dynamical absorption in dDNA as well as rare nonlinear phenomena such as resonant jumps and energy interactions between nonlinear modes" [6]. Solutions obtained for forced vibrations in dDNA oscillatory model [7] may correspond with process of binding the enzyme to the specific part of the DNA molecule. "Enzyme has a role of inducer of forced vibrations. In the transcription process only one chain is used as a template for transcription, the other chain is control. The part of DNA chain that is the template has to make more movements than the other chain. Dynamical absorption on the first pair of the main coordinates of the main chains appears on the resonant circular frequencies of the set of the double DNA helix chain system with one less pair of the material particles compared to the considered real system. Resonant state that appears only in one main chain may be important for selecting the specific sequence for transcription. We suggest that every sequence of DNA that encodes the specific protein has its own resonant circular frequencies different from the sequences that encode other proteins. Dynamical absorption on the second pair of the main coordinates of the main chains appears on the resonant circular frequencies of the set of the double DNA helix system with two less pairs of the material particles in comparison with considered system. This mathematical fact is important to consider in the light of the interruption or break of the double DNA helix system on the specific places where the transcription process starts and ends" [7].

"We are free to suggest that, from the mechanical point of view, if one specific frequency excitation caused by RNA polymerase is the same as eigen oscillatory frequency of specific promoter region resonance appears, that is the condition for starting the transcription from the mechanical point of view. This means that every gene has its specific "starting" oscillatory frequency that will correspond with one frequency external excitation. This may also correspond with spatially localized solitons in soliton –existence supporting models of DNA" [13].

"Expressions for the kinetic and potential energy as well as energy interaction between chains in the double DNA chain helix are obtained and analyzed for a linearized model [14]. By obtained expressions we concluded that there is no energy interaction between eigen main chains of the double DNA helix"[12].

Under certain sequences it is possible that oscillatory signal is transferred only through one chain.

"The results open possibilities for a different approach to explaining the behavior of the double chain DNA and of transfer of oscillatory signals trough the chains. Under certain sequences it is possible that oscillatory signal is transferred only through one chain. This may correspond to base pair order and translation process in complementary fractional order chains of DNA double helix in a living cell"[12].

We consider multi-pendulum models appropriate for experimental testing of visco-elastic properties of DNA [1].

## 3. An oscillatory model of a mouse zona pelucida (mZP)

**Summary.** The fertilization process on a cellular level of interaction can be considered as an oscillatory phenomenon. The surface of the interaction of the oocyte and sperm cell in IFV protocols is zona pelucida (ZP) - a complex network of polymers that has gel consistence, net like structure and can dynamically change its mechanical properties during the process of oocyte maturation, fertilization and early stage embryo. Its main biological function is selectivity regarding sperm penetration. We develop a single layer oscillatory net model of mouse ZP (mZP). The oscillatory spherical net model of mZP is a type of discrete systems based on oscillations in crossed chain systems. This model is suitable for explaining the process of fertilization- interaction of an oocyte and the spermatozoa and for studying the effect of oscillatory behavior of ZP regarding the influence of sperm impact angle, sperm velocity and sperm number. The model is further improved by proposing a multilayer model of ZP. The model can be used to analyze the energy state of ZP before and after fertilization. To better understand the interaction of oocyte and sperm cell the deformation work of ZP and parameters that influence it, a quasi-static continual shell-like ZP model was developed. The dynamics of frictional contact between the oocyte and the spermatozoa is studied by using the finite element method. Using phenomenological mapping of a model of ZP as a mechano-responsive and electroactive – polymer, a new mechano-chemical fertilization concept is proposed.

### 3.1. The oscillatory spherical net model of mouse zona pellucida. Mouse ZP structure is important for fertilization, polyspermy block, integrity of the growing embryo and guiding the embryo through the oviduct. In the late blastocyst stage, this structure no longer exists. During oocyte maturation, fertilization and embryo development ZP dynamically changes its elasticity.

Oscillatory spherical net model of mZP [16–18] was inspired by the Green modification of Wassermans' model of mZP [19] and 3D structural changes of ZP on atomic force microscopy [20–22] and scanning electron microscopy analysis [23]. We considered the oocyte with ZP as a biomechanical oscillator that could oscillate in free and forced regimes. We considered that a forced regime is induced by sperm cells that are "attacking" the outer surface layer of the oocyte- the ZP. The focus is on the events that are happening on the ZP, induced by impacts of sperm cells. First, a single layer model oscillatory spherical net model of mZP was developed.

Mouse ZP as a spherical net consists of orthogonal chains in meridian and circular directions with cross-sections with knot mass particles. Net envelopes the oocyte in one layer. The net has the same structure in circular and meridian directions and lies in the sphere concentric to the oocyte that we suppose is rigid.

Each oscillatory mechanical chain has a finite number of material particles with a finite number of degrees of freedom. Chains are composed of material particles of different masses interconnected with massless non-linear elastic elements on a specific manner. See Fig 3. a and b. For modelling this oscillatory spherical net of mZP, the method of discrete continuum was used [24]. Each material particle has three degrees of freedom and is connected to the sphere surface with a standard light non-linear-elastic element in the radial direction and can oscillate in the radial, circular and meridional directions. We suppose that, from the mechanical point of view, fertilization occurs in the moment of forced regime of oscillations of mZP induced by sperm cells, when a spermatozoid that oscillates in a resonance with the ZP net, penetrates the ZP.

The resonant frequencies for a certain theoretical initial conditions are determined using the frequency equation:

$$f(\omega^2) = \left| C - \omega^2 A \right| = 0 \tag{2}$$

C is a matrix of coefficients of elasticity, and A is a matrix of coefficients of inertia. The numerical analyses were done on a representative part of the mZP network that still preserves the molar ratio of the ZP glycoproteins (ZP1, ZP2 and ZP3). The frequency equation is an eleven-degree function.

**The assumption of the model**: the system of ZP oscillatory net oscillates in a free regime after ovulation without presence of spermatozoa. If there is only an initial perturbation by kinetic and potential energy given to oscillatory structures, only free vibration regimes of vibration discrete structure appear. In this case material particles at the initial moment obtain the initial displacement measured from their equilibrium positions and initial velocities. The conditions for free oscillations is that only one mass particle position is perturbed from its equilibrium position, or that only one mass particle at its equilibrium position obtains initial velocity.



a*        b*        c*
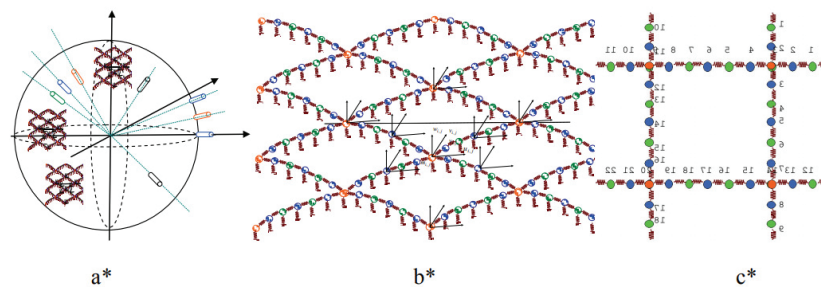
FIGURE 3. a* Model of ZP spherical surface that shows a radial direction of axis of constructive elements of the model - ZP proteins. b* Part of the ZP network on a part of the sphere (oocyte). Orange (ZP1), blue (ZP2) and green (ZP3) represent ZP proteins. The network is identical in both circular and meridional direction. Axis shows directions of movements of ZP proteins. Each ZP protein is connected to the sphere with elastic springs that can oscillate in radial direction. c* segment of spherical surface net model of mZP. Taken from [17].

The bonds between the molecules that form the chains can be ideally elastic or viscoelastic depending on the state in which the biological system is. By applying analytical methods, the values of the natural frequency of oscillation of nodal -ZP1 molecules were obtained. ZP1 molecules have been selected for two reasons – their masses are the largest thus their contribution to the oscillatory behavior will be significant; upon fertilization, by creating disulphide bridges between ZP1 molecules on one side and ZP2 and ZP3 on the other, followed by a change of ZP structure, Young modulus of elasticity increases [25] and the conditions for a polyspermy block are created. In addition, according to the modified Wassarman model of ZP [26], without the ZP1 bonding molecules the net structure of ZP does not exist [27, 28].

If the system of ZP net is considered linear and conservative, free oscillations of mZP molecules in radial $w_{ij}$ circular $u_{i,j}$ and meridian $v_{i,j}$ direction can be described by a system of homogeneous linear differential equations in the following form:

$$m_{ij}\ddot{w}_{ij} = -c_{(w)ij}w_{ij} \tag{3}$$

$$m_{ij}\ddot{u}_{ij} = +c_{(u)ij}\left(u_{i+1.j} - u_{i.j}\right) - c_{(u)i-1,j}\left(u_{i.j} - u_{i-1.j}\right) \quad . \tag{4}$$

$$m_{ij}\ddot{v}_{ij} = +c_{(v)i,j}\left(v_{i.j+1} - v_{i.j}\right) - c_{(v)i,j-1}\left(v_{i.j} - v_{i.j-1}\right) \quad . \tag{5}$$

The system of linear differential equations (3), (4) and (5) corresponds to the situation before fertilization if we supposed that the initial perturbation of the position and velocities from the equilibrium is caused by ovulation.

Forced oscillations of mZP that is considered as a linear conservative system that oscillates under external multi-frequency force can be described by the following system of nonhomogeneous linear differential equations:

$$m_{ij}\ddot{w}_{ij} = -c_{(w)ij}w_{ij} + F_{i,j}\cos\left(\Omega_{ij}t + \alpha_{ij}\right) + \tilde{F}_{i,j}\cos\left(\tilde{\Omega}_{ij}t + \tilde{\alpha}_{ij}\right) \tag{6}$$

$$m_{ij}\ddot{u}_{ij} = +c_{(u)ij}\left(u_{i+1.j} - u_{i.j}\right) - c_{(u)i-1,j}\left(u_{i.j} - u_{i-1.j}\right) \quad . \tag{7}$$

$$m_{ij}\ddot{v}_{ij} = +c_{(v)i,j}\left(v_{i.j+1} - v_{i.j}\right) - c_{(v)i,j-1}\left(v_{i.j} - v_{i.j-1}\right) \quad . \tag{8}$$

The system of linear differential equations (6), (7) and (8) corresponds to the situation just before fertilization when sperm cells influence the ZP surface in continual and successive manner. The assumption is that sperm cells have periodic discontinued contact with ZP net.

Forced oscillations of the nonlinear non-conservative system of oscillating ZP net can be described by a system of nonhomogeneous non-linear differential equations:

$$m\ddot{w}_{ij} = -c_{(w)}w_{ij} - \tilde{c}_{(w)}w_{ij}^3 - b_{(w)ij}\dot{w}_{ij} + F_{i,j}\cos\left(\Omega_{ij}t + \alpha_{ij}\right) + \tilde{F}_{i,j}\cos\left(\tilde{\Omega}_{ij}t + \tilde{\alpha}_{ij}\right) \tag{9}$$

$$m\ddot{u}_{ij} = +c_{(u)}\left(u_{i+1.j} - u_{i.j}\right) + \tilde{c}_{(u)}\left(u_{i+1.j} - u_{i.j}\right)^3 - c_{(u)}\left(u_{i.j} - u_{i-1.j}\right) - \tilde{c}_{(u)}\left(u_{i.j} - u_{i-1.j}\right)^3. \tag{10}$$

$$m\ddot{v}_{ij} = +c_{(v)}\left(v_{i.j+1} - v_{i.j}\right) + \tilde{c}_{(v)}\left(v_{i.j+1} - v_{i.j}\right)^3 - c_{(v)}\left(v_{i.j} - v_{i.j-1}\right) - \tilde{c}_{(v)}\left(v_{i.j} - v_{i.j-1}\right)^3. \tag{11}$$

The system of non-linear differential equations (9), (10) and (11) corresponds to the situation after fertilization when for the very short time other sperm cells affect the ZP surface.

For obtaining solutions of displacements of molecules, known solutions of linear homogeneous differential equations obtained by trigonometric methods [29] was

used. Solutions for oscillatory movements in radial directions for ZP1 molecules are:

$$w_{ij}(t) = A_{(w)ij} \cos\left(\omega_{(w)0}t + \alpha_{(w)ij}\right) \tag{12}$$

$A_{(w)ij}$ is amplitude, $\alpha_{(w)ij}$ phase of single frequency force, $\omega_{(w)0} = \sqrt{\dfrac{c_{(w)}}{m}}$ is circular frequency $c_{(w)}$ is rigidity of connections between molecules. Proposed solutions for system of linear homogeneous differential equations (3) and (4) are in the following form:

$$u_{ij}(t) = A_{(u)ij} \cos\left(\omega_{(u)j}t + \alpha_{(u)j}\right) , \tag{13}$$

$$v_{ij}(t) = A_{(v)ij} \cos\left(\omega_{(v)i}t + \alpha_{(v)i}\right) \tag{14}$$

Where amplitudes $A_{(u)ij}$ and $A_{(v)ij}$ have the following form:

$$A_{(u)ij} = C_{(u)j} \sin i\varphi, \quad A_{(v)ij} = C_{(u)i} \sin j\vartheta. \tag{15}$$

• Component displacements in meridian and circular directions of knot molecules are multi-frequency oscillations. Depending on initial perturbation of the equilibrium state of material particles in the spherical net, component displacements of knot mass particles are in multi-frequency oscillatory regimes, but with number of frequencies less or equal to the number of eigen frequencies of the system. The analysis of oscillatory behavior of knot molecules in mZP spherical net model are done through generalized Lussajous curves. The resulting trajectory of the component motions in the circular and meridian directions in the plane tangential to the sphere net of the observed ZP1 molecules in the model are in the form of generalized Lissajous curves that could be in the form of a strait line, periodical, non-periodical, stochastic-like or chaotic-like trajectories, as a results of summing two orthogonal multiple-frequency component vibrations. For obtaining a real space trajectory of a knot mass particle, the components in radial direction have to be added [30]. Fig. 4. Numerical methods were used to obtain amplitude-frequency graphs of oscillation of ZP1 molecules depending on the speed, angle of action, and number of spermatozoa [30–32]. ZP1 molecule is the main cross-linker of the 3D ZP net structure and response for hardening effect of ZP after fertilisation [19, 33]. On the basis of the shape of Lissaous curves, a frequency analysis of the behavior of molecules in the oscillatory model of ZP was performed. Comments related to successful fertilization are given by analysing the oscillatory behavior of molecules. Angles at which sperm acts upon ZP surface affects its oscillatory behaviour. Some angles are more favourable for achieving oscillatory stats favourable for fertilisations [31, 34]. The authors suggested that for the successful fertilisation favourable are sperm impact angles that result in synchronisation of mZP net molecules. Very small and very large impact angles are unfavourable; fertilization [30].

Generalized Lissajous curves on Fig 4b has chaotic –like form showing that the π/2 sperm impact angle is not suitable for fertilization. It is the most unfavorable impact angle, although the amplitudes of motions of knot molecules are very low.

The number of sperm cells with effective swimming velocity, capable of reaching the oocyte and undergoing complex adaptations within the female reproductive tract is a key determinant of male fertilization success [35]. The quality of the whole ejaculate is important for the fertilization success. Total sperm numbers are positively correlated to proportions of normal sperm, acrosome integrity and motile sperm and also with gonadosomatic index [36]. ZP1 molecules in the mZP oscillatory model have different oscillatory states when exposed to external vibro -impacts of a different number of hyperactivated spermatozoa, indicated that a certain number of hyperactivated spermatozoa is necessary for reaching the favorable oscillatory state of mZP for fertilization [32]. Influence of the sperm velocity on oscillatory behavior of mZP was studied in [31]. The important result of numerical analysis is that oblique angles are more favourable and this was also suggested in [37]. Using the oscillatory spherical net model of mZP, it is possible to predict values of sperm impact angles favourable for fertilization.
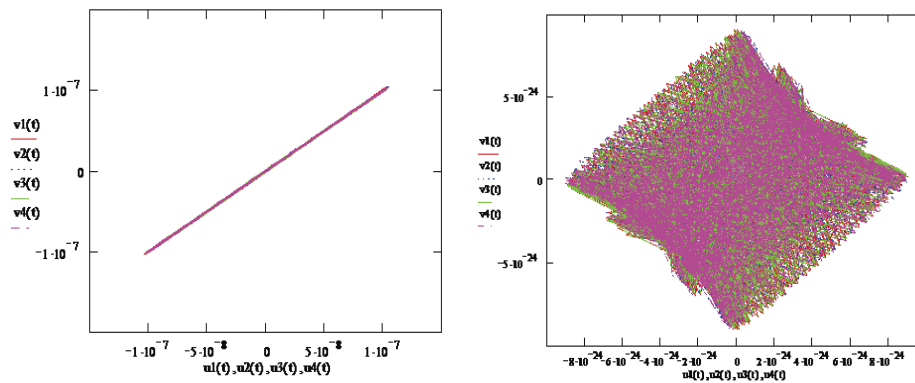


FIGURE 4. a. Full synchronization (angles $\pi/6$ and $\pi/4$). b. Full asynchronization for (angles $\pi/2$ and $\pi/2$) of all four ZP 1 molecules from representative part of the mZP oscillatory net.

The model is suitable for modelling and explaining the different conditions that this structure goes through during oocyte maturation and after fertilization [38]. The generalized function of dissipating the total energy of the oscillatory system of mZP, and the representative part of the network, is derived. Fig 5. An interpretation of the dynamic changes in the elastic properties of mouse ZP and the energy dissipation that occurs after fertilization and its potential biological significance is given in [38]. "The energy state of the mouse zona pellucida before and after fertilization has been analysed via the created discrete fractional order spherical net model based on the fractional derivative Voigt model of viscoelasticity. According to this model, after fertilization, until the stage of morula the modulus of elasticity decreases [27], and these stages could be modelled as non-conservative systems with viscoelastic properties.
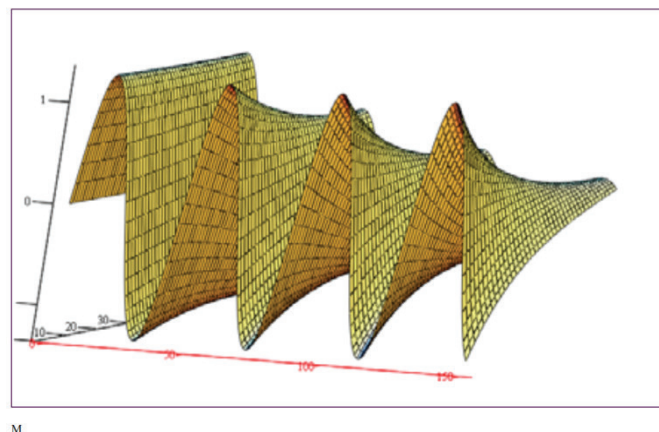
Figure 5. Main eigen modes of fractional order representative part of mZP net, $T_{s,sin}(t,\alpha)$ is plotted on the ordinate, time t and $\alpha$ ($0 < \alpha \leq 1$) are on two abscissa axes. Taken from [38].

In the stage when the mZP has the highest viscosity, its energy is minimal. We can speculate that this minimum of mZP energy is essential (from the mechanical point of view) for embryo to escape from this structure and implant itself into the uterus." [38].

Our analysis of influence of sperm impact angle on parametric frequency analysis of oscillatory behaviour of knot molecules in mZP spherical net model is one step forward in understanding dynamical conditions and vibro-impacts in the process of mammalian fertilization and the process of polyspermy block [11].

**Synchronisation of oscillations of mZP molecules.** The phenomenon of synchronisation and desynchronization of mZP1 molecules using multi-parametric analysis is studied in [39]. One or more parameter transformations of curve graphs in the phase space of the oscillatory state of the kinetics of one or more molecules using combinations of oscillatory displacements of one or more molecules in the radial and/or circular direction can be followed. The results are analysed in the context of polyspermy block. The polyspermy block is a phenomenon that includes electrical and mechanical events on ZP structure caused by sperm penetration trough ZP. The result is that other sperms could neither attach to nor penetrate the ZP [40]. One of the theories is that chemical modifications of ZP2 and ZP3 molecules are responsible for polyspermy block [33]. Polyspermy block is the mechanism that ensures the constant quantity of genetic material in each generation. Based on the results of the numerical experiment on the viscoelastic oscillatory model of mouse ZP after fertilization, we notice that mZP1 molecules oscillate synchronously when the bonds between them are stronger (higher values of linear and nonlinear stiffness coefficients) and when the system damping is more pronounced. Experimental data show that the higher viscosity of ZP after fertilization is associated with a more efficient polyspermy block and embryo survival [39, 41]. Based on these data, we

can assume a connection between the synchronization of the oscillatory motion of ZP molecules and polyspermy block: better synchronization could mean more efficient polyspermy block.

**Limitation of the oscillatory spherical net model of mZP. The main limitations are***: the analysis of oscillatory behaviour were done on a representative part of the mZP net and that model is a single-layer model. In the real ZP there are numerous ZP molecules and so the numerous eigen circular frequencies. Non-linear properties of real ZP and limitations of the analytical method of solving a system of differential non-linear equations require using numerical methods and approximations in modelling. Real ZP is a very complex oscillatory system and very selective in regard to spermatozoa penetration. This ZP selectiveness provides constant quantity of genetic material in each generation.

In order to overcome some limitations of the one-layer oscillatory spherical net model of mZP a multi-layered model is developed [42].

## 3.2. Multi-layer oscillatory spherical net model of mouse zona pelucida.

On a basis of single-layered oscillatory spherical net model of mZP we proposed improved double layer models [42]. Due to visco-elastic properties of ZP and its importance for mechanism of sperm penetration double layered oscillatory net model of mZP has fractional order properties. Fig. 6. In the double-layered mZP oscillatory model interconnections between ZP glycoproteins have fractional order properties. In this way, oscillatory behavior of ZP from pure elastic to viscous is covered. A double-layered model with fractional order properties has advantage over a single-layered model with ideally elastic properties because it can explain changes in ZP mechanical properties before, in the course of and after fertilization [22, 43]. Assuming that both layers have identical regular geometry and structure, examples of double-layered oscillatory networks are presented in Fig 6. Each molecule is interconnected with two neighboring molecules and with ZP surface with standard light fractional order visco-elastic elements. At places where upper and lower net are overlapped (not molecules or ZP2 molecules as in Fig 6), nets are interconnected by these molecules with standard light fractional order visco-elastic elements.

Lower net is rotated for an angle of 45° compared to the upper net overlapping the knot molecules at one diagonal. Sides of the square of upper spherical net corespond to the diagonal of the square of the lower spherical net. In the undeformed state, interconection lengths are longer in upper than in the lower net making that fenestrations of upper net larger than those of the lower. This assumtion coresponds to experimental results [23, 44]. Using a double-layered oscillatory fractional order ZP net, it is possible to explain the mechanism of sperm penetration trough ZP. Sperm cells have a more demanding task of passing through a denser environment than in the case of the single-layered net. I*n vitro* [37] and numerical [30] experiments have reported that sperm creates an oblique path through ZP. Double-layered oscillatory fractional order ZP net model gave basis that possible mechanism of sperm penetration trough ZP are oscillations of relaxations.

A system of ordinary fractional order differential equations for fractional order oscillations of chains with 11 molecules (material particles) of a representative

segment of *lower (inner)* spherical net are in the following form:

for molecules in chains in circular direction:

$$m_{k,j}\ddot{u}_{k,j}(t)+c_{0(k-1,k),j}\left[u_{k,j}(t)-u_{k-1,j}(t)\right]-c_{0(k,k+1),j}\left[u_{k+1,j}(t)-u_{k,j}(t)\right]+c_{0\leq\alpha\leq1(k-1,k),j}\mathfrak{D}_t^\alpha\left[u_{k,j}(t)-u_{k-1,j}(t)\right]-$$
$$-c_{0\leq\alpha\leq(k,k+1),j}\mathfrak{D}_t^\alpha\left[u_{k+1,j}(t)-u_{k,j}(t)\right]=0$$
$$k=1,2,3,\ldots,\mathbf{1}\quad,j=1,3,\ 0\leq\alpha\leq1 \tag{16}$$

for molecules in chains in meridian direction:

$$m_{k,j}\ddot{v}_{k,j}(t)+c_{0(k-1,k),j}\left[v_{k,j}(t)-v_{k-1,j}(t)\right]-c_{0(k,k+1),j}\left[v_{k+1,j}(t)-v_{k,j}(t)\right]+c_{0\leq\alpha\leq1(k-1,k),j}\mathfrak{D}_t^\alpha\left[v_{k,j}(t)-v_{k-1,j}(t)\right]-$$
$$-c_{0\leq\alpha\leq(k,k+1),j}\mathfrak{D}_t^\alpha\left[v_{k+1,j}(t)-v_{k,j}(t)\right]=0$$
$$k=1,2,3,\ldots,\mathbf{1}\quad,j=2,4,\ 0\leq\alpha\leq1 \tag{17}$$

for all molecules of inner net except knot molecules (mZP1) and for knot molecules that are not interconnected to the upper (outer) net knot molecule:

$$\widetilde{m}_{k,j}\ddot{w}_{k,j}(t)+\widetilde{c}_{0(k,j),j}w_{k,j}(t)+c_{0\leq\alpha\leq1(k,j)}\mathfrak{D}_t^\alpha\left[w_{k,j}(t)\right]=0\ k,j=1,2,3,\ldots,\mathbf{1}\ ,\quad k\neq3,\quad k\neq9\ ,$$
$$0\leq\alpha\leq1 \tag{18}$$

for knot molecules (mZP1) that interconnect inner and upper net and are connected to the ZP surface by standard light fractional order elements:

$$\widetilde{m}_{k,j}\ddot{w}_{k,j}(t)+\widetilde{c}_{0\ (k,j),j}w_{k,j}(t)-\widetilde{c}_{0(k,j),j}\left[\widetilde{w}_{k,j}(t)-w_{k,j}(t)\right]-\widetilde{c}_{0\leq\alpha\leq1(k,j)}\mathfrak{D}_t^\alpha\left[\widetilde{w}_{k,j}(t)-w_{k,j}(t)\right]+$$
$$+\widetilde{c}_{0.0\leq\alpha\leq1(k,j)}\mathfrak{D}_t^\alpha\left[w_{k,j}(t)\right]=0$$
$$k=3,\quad or/and\ k=9,\quad j=3,\quad or/and\ j=9,\ 0\leq\alpha\leq1 \tag{19}$$

$$\widetilde{\widetilde{m}}_{k,j}\ddot{\widetilde{w}}_{k,j}(t)+\widetilde{c}_{0(k,j),j}\left[\widetilde{w}_{k,j}(t)-w_{k,j}(t)\right]+\widetilde{c}_{0\leq\alpha\leq1(k,j)}\mathfrak{D}_t^\alpha\left[\widetilde{w}_{k,j}(t)-w_{k,j}(t)\right]=0$$
$$k=3,\quad or/and\ k=9,\quad j=3,\quad or/and\ j=9,\ 0\leq\alpha\leq1 \tag{20}$$

The system of ordinary fractional order differential equations for fractional order oscillations of chains with 11 molecules of the representative segment of *upper* (outer) spherical mZP net is in the following form (see Fig. 3):

For molecules in chains in circular direction (at angle of 45° compared to lower net circular chain):

$$m_{k,j}\ddot{\widetilde{u}}_{k,j}(t)+c_{0(k-1,k),j}\left[\widetilde{u}_{k,j}(t)-\widetilde{u}_{k-1,j}(t)\right]-c_{0(k,k+1),j}\left[\widetilde{u}_{k+1,j}(t)-\widetilde{u}_{k,j}(t)\right]+c_{0\leq\alpha\leq1(k-1,k),j}\mathfrak{D}_t^\alpha\left[\widetilde{u}_{k,j}(t)-\widetilde{u}_{k-1,j}(t)\right]-$$
$$-c_{0\leq\alpha\leq(k,k+1),j}\mathfrak{D}_t^\alpha\left[\widetilde{u}_{k+1,j}(t)-\widetilde{u}_{k,j}(t)\right]=0$$
$$k=1,2,3,\ldots,\mathbf{1}\ ,\ j=1,3,\ 0\leq\alpha\leq1 \tag{21}$$

For molecules in chains in meridian direction (at angle of 45° compared to lower net meridian chain):

$$m_{k,j}\ddot{\widetilde{v}}_{k,j}(t)+c_{0(k-1,k),j}\left[\widetilde{v}_{k,j}(t)-\widetilde{v}_{k-1,j}(t)\right]-c_{0(k,k+1),j}\left[\widetilde{v}_{k+1,j}(t)-\widetilde{v}_{k,j}(t)\right]+c_{0\leq\alpha\leq1(k-1,k),j}\mathfrak{D}_t^\alpha\left[\widetilde{v}_{k,j}(t)-\widetilde{v}_{k-1,j}(t)\right]-$$
$$-c_{0\leq\alpha\leq(k,k+1),j}\mathfrak{D}_t^\alpha\left[\widetilde{v}_{k+1,j}(t)-\widetilde{v}_{k,j}(t)\right]=0$$
$$k=1,2,3,\ldots,\mathbf{1}\ ,\ j=2,4,\ 0\leq\alpha\leq1 \tag{22}$$

where $u_{k,j}(t)$, $v_{k,j}(t)$ and $w_{k,j}(t)$ are molecule component displacements in circular, meridian and radial directions of the representative segment of lower net,

$\widetilde{u}_{k,j}(t)$, $\widetilde{v}_{k,j}(t)$ and $\widetilde{w}_{k,j}(t)$ are molecule component displacements in circular, meridian and radial directions of the characteristic, representative segment of the upper net, $\mathfrak{D}_t^\alpha[\bullet]$ is a fractional order differential operator of the $\alpha^{th}$ derivative with respect to time $t$ .
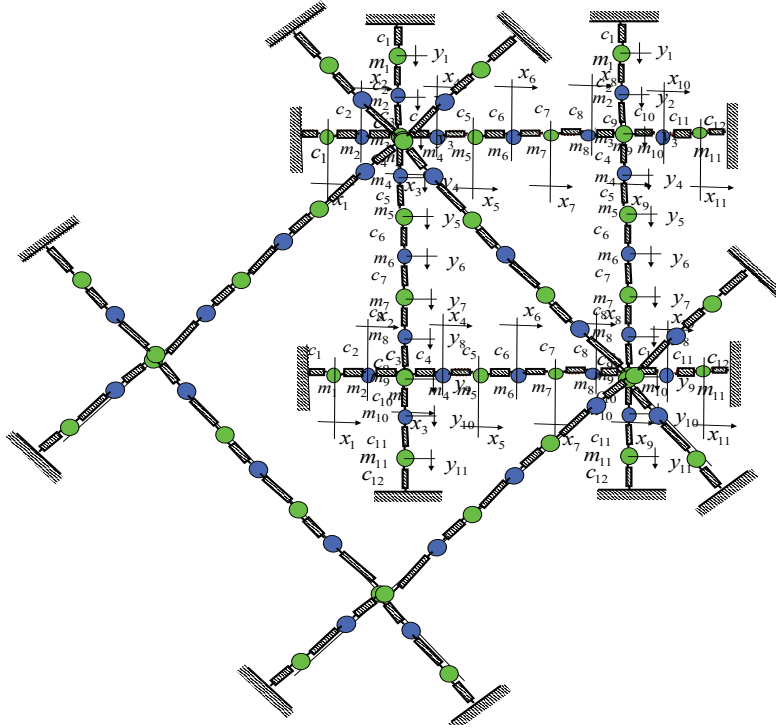


FIGURE 6. Part of double-laired net in oscillatory spherical net model of mZP with fractional properties-possible arrangement. Taken from ref [42].

Influence of the sperm impact angle on local sperm oocyte contact dynamics was analysed using a finite element method approach [45]. Sperm–oocyte contact was defined as a non-linear frictional contact. Deformations of ZP relative to different sperm impact angles are analysed. An effect which resembles the "slip-stick" effect was identified. Spermatozoa accelerate and decelerate during the sliding on the ZP surface and this is characteristic to slip – stick motion. Some favourable ZP-stress state for sperm penetration for different sperm impact angles are also identified. [45]. The sperm head–ZP contact area increases as sperm impact angle decreases [45]. Spermatozoa with sperm impact angle of $75^0$ achieves local maximum equivalent stress in ZP and has the maximum contact area. Spermatozoa with sperm impact angle of $10^0$ achieves maximum total deformation, frictional stress and sliding distance. The analysis [45] revealed local minimums and local maximums of maximum equivalent ZP stress, maximum contact pressure, total contact stress

and frictional stress for certain sperm impact angles. Local maximums of maximum equivalent ZP stress are for sperm impact angles 40°, 60°, 75° respectively, with the maximum value for sperm impact angle of 75°. Local minimums of maximum equivalent ZP stress are for sperm impact angles 10°, 30°, 50°, 70°, 90° with a minimal value for $10^0$ [45]."Although it was expected that the maximum equivalent stress in the local contact zone of ZP would be obtained for the angle of 90°, the simulation results showed otherwise." [45].This is probably that penetration force has two components-tangential and radial components. Tangential component is equal to the sliding friction force that resists the spermatozoa head movement on the ZP surface. For a sperm impact angle of 90°, the frictional forces are minimal due to absence of tangential force component [45]. For a sperm impact angle of 10° at the end of the simulation time, sperm velocity is higher than it is for sperm impact angles above 10° (30°, 60°, 90) [45]. Similar experimental results were obtained by [46] suggesting that, sperm develops a strategy to overcome this ZP reaction by decreasing its velocity over time. Maximum equivalent stress of ZP is predominantly induced by spermatozoa propulsion force [45].

## 3.3. The influence of sperm velocity on oscillatory behaviour of mZP.

The model of oscillatory spherical net of mouse ZP was used for the analysis how the sperm velocity and arrangement upon the ZP surface affect the oscillatory behavior of mZP [31]. It is universally acknowledged that the success of fertilization is measured by the quality of spermatozoa, primarily by the percentage of progressively moving spermatozoa. In the course of fertilization in both in vivo and in vitro conditions, oocyte is in contact with spermatozoa of different quality (morphology, velocity, acrosome status). ZP is a mechanosensitive structure and response on mechanical stimulation that come from sperm on its surface.

Acting upon the surface of ZP all these spermatozoa, each in its own way, contribute to the change of oscillatory behavior of the ZP and oocyte as a whole. Their joint action contributes to the final result – fertilizationThe oscillatory pattern is different for healthy spermatozoa and spermatozoa having morphological defects [47]. Thus, action of spermatozoa having different characteristics can be considered as action of external periodic forces having different characteristics.

Different distributions of spermatozoa having the same/different kinetic parameters result in different distributions of external forces acting on the ZP surface. Each individual spermatozoid generates certain force which acts upon the ZP surface [48] and their joint action will give specific distribution of force on the ZP surface. A symmetric or asymmetric distribution of force produced by action of spermatozoa upon ZP surface will cause different oscillatory states of the ZP. Theoretically, there are combinations of the distribution of this force resulting in the same or similar oscillatory states of the ZP. Examples of different distributions of spermatozoa on the ZP surface are shown in Figs. 7 A, B, and C.

For numerical analysis only, spermatozoa with effective velocities were used [49]. The numerical simulations show that for the cases when a symmetric distribution of spermatozoa having the same velocity exists, the resulting trajectories of the

knot molecules in the plane tangential to the spherical surface have the form of a straight line, -they move synchronously, only amplitudes of these movements are different depending upon the angle of impact of the spermatozoa action [31]. "Under physiological conditions, slow spermatozoa would never reach the oocyte, but in IVF conditions they could contribute to creation of a favourable oscillatory state of mZP." [31].
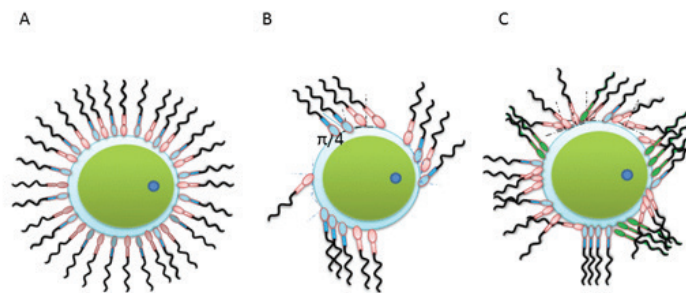


FIGURE 7. Hypothetical arrangement of spermatozoa on ZP surface: A Symmetrical arrangement of spermatozoa having two different swimming velocities. B Asymmetrical arrangement of spermatozoa having two different swimming velocities but the same impact angle. C Asymmetrical arrangement of spermatozoa having three different swimming velocities and different impact angles arbitrarily arranged. Different colors of spermatozoa (pink, blue or green) denote their different swimming velocities. Taken from ref [31].

Under specific initial conditions, it is possible that only individual knot molecules in the model move along a straight line in the plane tangential to the sphere surface, while the others do not. The possibility that some knot molecules oscillate synchronously while the others do not, indicates that the fertilization phenomenon could have a local character, indicating that the position of the initial penetration of spermatozoa through ZP could be determined by local initial conditions which are of stochastic character while the structure and composition of the ZP surface could be assumed to be uniform.

This research opened some questions regarding the relation between kinetic parameters of sperm swimming velocity and sperm impact angle, and the arrangement of sperm cells with effective velocity on the mZP surface.

Considering the fertilization process as an oscillatory phenomenon, and the mZP as an oscillatory structure, we supposed that the oocyte and embryo are in different oscillatory states [50] and that the whole cell and ZP structure have different energies.

The double-layered model is suitable for explaining the mechanism of penetration of spermatozoa trough ZP thickness on a basis of oscillations of relaxations and

could serve as the basis for the next more complex model of mZP where mZP will be considered as an oscillating gel. By modelling mZP as an oscillating gel, it will be possible to investigate nonlinear dynamical phenomena that can arise from the coupling of mechanical and chemical energy"[51]. Regarding the limitations of the oscillatory spherical net MZP model, specifically that the fertilization process includes not only the biomechanical events, but also the physico-chemical, electro- and thermal effects which are coupled, a novel concept that the ZP can be modelled as a mechano-responsive gel is given in [52].

## 3.4. Zona pelucida as a mechano-responsive polymer. Temperature, pH and ionic strength influence biological function of ZP and its aggregate state. We consider ZP as a mechano-responsive polymer and propose a new theory of fertilization based on coupled chemical—electrical fields and modelled ZP as a non-linear oscillatory reactive system [52]. Analysis of its oscillatory states regarding external force is discussed in [52]. The process of oocyte fertilization requires a certain amount of functionally capable spermatozoa, although only one sperm will fertilize the oocyte ensuring the constant quantity of genetic material in each generation. In this system, oocyte is reacting as an inert body due to huge differences in cell masses between spermatozoa and oocyte (in range of $10^7$). From the oscillatory theory of fertilization [53] ZP changes its oscillatory states after fertilization [16, 54] as well as mechanical properties [27]. Changes in mechanical and electrical properties after fertilization allow attaching of silicon nano chips [55]. ZP is a polymer with highly sulfated glycoproteins interconnected with non-covalent bonds, so it is easily dissolved by mild heating, low pH, low ionic strength [26]. In this model ZP is considered as a mechano-responsive but also electroactive – polymer analogue to [56, 57]. Using phenomenological mapping [11, 58], concept of controlling chemical oscillations in mechano reactive gels [57, 59] and consequent rhythmical soluble-insoluble changes of the gel [60] the new mechano-chemical fertilization concept is proposed. The system (ZP) is considered to be incompressible. "Oscillations in chemical reactions are possible to control via mechanical strain [57, 59]. Basic assumptions: Sperm penetration area is determined by local parameters acting upon ZP surface. ZP surface is negatively charged due to content of sulphated glycoproteins. Numerous sperms with different velocities and different sperm impact angles act upon ZP surface in a form of periodic impulsive forces transferring a part of their kinetic energy to the ZP structure. This external mechanical influence (time dependent force intensity and pressure changings) of spermatozoa cause changing in chemical reaction (analogue to [57, 59]that change the local pH of ZP causing local changes of its aggregate state (analogue to [60]) from soluble to insoluble or causing the state of plastic flow of ZP. The area of ZP where the plastic flow persists long enough will be the "weak spot/area" for sperm penetration. The spermatozoid that is in range of this area could easily swim through ZP. By changing the local parameters of the external mechanical force (stress intensity, pressure, sperm arrangement...) it is possible to control local chemical oscillatory processes [59]. Further,

receptor recognition between sperm and oocyte changes the local potential of cell membranes. According to the proposed model of the fertilization process, ZP is an area of coupled mechano-electro-chemical fields. The approximation is that this phenomenon has a local character and that it is not uniform through the entire ZP." [52]. Fig 8. In light of the coupled field theory, we suggest a possible role of cortical granules of the oocytes (CG): content of CG (mostly enzymes) are acting like catalysts to chemical reactions in the sense that they change the pH of the local environment. The changed pH than changes the conformation of the ZP glycoproteins and discloses additional bounding sides on ZP glycoproteins leading to its structural reorganization.
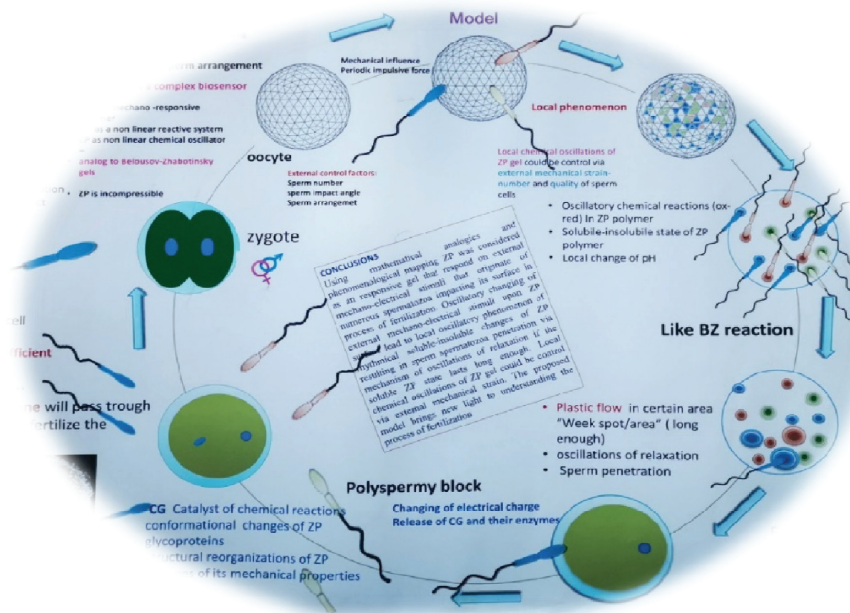


FIGURE 8. Zona pelucida as a mechano-responsive polymer. ZP is considered as a responsive gel that responds to external mechano-electrical stimuli that originate from numerous spermatozoa impacting its surface in the process of fertilization. Oscillatory changing of external mechano-electrical stimuli upon ZP surface lead to a local oscillatory phenomenon of rhythmical soluble-insoluble changes of ZP resulting in penetration by a spermatozoid via a mechanism of oscillations of relaxation if the soluble ZP state lasts long enough. Local chemical oscillations of ZP gel could be controlled via external mechanical strain.

## 3.5. Other approaches to modeling the sperm-oocyte dynamics. "Using the quasi-static approximate ZP model in the form of a hollow sphere the numerical analysis of how specific deformation work depends on different variables like: ZP thickness, specific point in ZP, external pressure that comes from sperm cells

were done in[61]. According to the model, spermatozoa that make pressure upon ZP surface are in the form of homogeny discrete continuum distribution in radial directions" [61]. The impact of spermatozoa upon ZP surface is not only mechanical but also involves a receptor-recognition mechanism. Specific deformation work could be used as a criterion for determining the point/area of ZP where spermatozoid penetration could occur. The point/area where the specific deformation work has the lowest values will be the area of the highest probability for sperm penetration. This point/area could be the "weak spot." ZP thickness is an independent parameter that affects the success of In vitro fertilization (IVF) protocols: the thicker the ZP is (smoking, age of female partner, serum levels of follicle-stimulating hormone (FSH) [62], the lower the probability for conception." Numerical analysis shows that volume dilatation-compression in thicker ZP would have lower values. This indicates that in thicker ZP volume dilatation/compression obtained by certain amount of sperm cells could not reach critical value for sperm penetration. As the ZP thickness increases the higher absolute values of volume dilatation – higher compression of ZP would be necessary/or the higher force/energy is needed to sperm to penetrate trough ZP thickness. Theoretically, sperm cell needs more energy to penetrate thicker ZP [63].

Microscope imaging techniques could be useful for testing whether sperm impact angles favourable for successful fertilization predicted by oscillatory spherical net ZP model [34] and finite element method of modelling frictional contact between the sperm cell and the oocyte are indeed the most favorable [45]. We believe that this oscillatory approach could contribute to the better understanding of the fertilization process: how oocyte makes selection through its extra-cellular matrix; that receptor-mediated mechanism of recognition and fertilization has an oscillatory phenomenon in its nature like resonance between oscillatory regimes of ZP and "chosen" sperm cell as a necessary condition for fertilization. "According to our oscillatory model, we are free to suggest a new type of treatment for male sub fertility: we believe that adding adequate mechanical stimulation in the medium with healthy oocyte and adequate number of spermatozoa could improve fertilization. Mechanical simulation could be in the form of a sound. The basic idea is that adding the mechanical stimulation with specific parameters (intensity and set of oscillatory frequencies) could contribute to achieving successful fertilization through the creation of resonance in the oscillations between an oocyte and a spermatozoid. This method could be useful in subfertility cases (when there are not enough spermatozoa with normal function and morphology to achieve fertilization in physiological conditions)" [31].

## 4. An oscillatory model of mitotic spindle

**Summary.** Each cell with a nucleus possesses a mitotic spindle -a complex molecular machinery responsible for the cell division process. It is necessary to devide genetic material, condense it in the form of chromosomes, from mother cell into daughter cells, equally. Specific movements of chromosomes during the stages of cell division process was an inspiration for developing a biomechanical oscillatory model of mitotic spindle that will be presented in this part of the manuscript. The

basic concept of the model with its assumptions will be presented. The idea that the resonance as a possible mechanism of separation of homologue chromosomes during anaphase is suggested. We postulated that the energy of oscillatory movements of chromosomes during meta- and anaphase of cell division cycle could be valuable physical parameters for estimating the energy balance within the cell. Potential, kinetic and total mechanical energy of pairs of dyads of sister chromatids regarding mass distribution of chromosomes, as well as the spindle size and the centrosome frequency are analysed. All these parameters affect the energy of the dyads of sister chromatids. Our model can be analysed as a visco-elastic system with linear dissipation of energy of the system, and also as a fractional order type system with fractional order dissipation energy. Fractional order forced oscillatory modes of elements of the mitotic spindle are presented. Different distributions of energy in the system of the mitotic spindle could represent an additional level of information coding that is transferred into the next cell generation and could be of interests in the process of cell differentiation. The model could be suitable for explaining the irregularities in cell division process in cancerogenesis.

During the cell division process, chromosomes –the carriers of genetic material move within the cell in a specific way, not just in interphase but also in the metaphase stage of the cell division cycle showing functional character in spatial, temporal and cell type specific organization [64, 65]. There are biomechanical models that describe dynamics of microtubules in the mitotic spindle [66]. These models are oriented on microtubules micro-dynamics and involved modelling of motions of specific proteins that form microtubules. There are many biomechanical models of the mitotic spindle[66–70]. In this part we will present a new approach in modelling dynamics of the mitotic spindle.

### 4.1. A biomechanical oscillatory model of mitotic spindle. A detail description of the biomechanical model of mitotic spindle is given in [71, 72]. Schematic representation of the basic concept of the biomechanical model of mitotic spindle is given in Fig. 9. The oscillatory behavior of this model is based on dynamics of coupled systems [73]. Mitotic spindle is considered as a system of coupled oscillators. The coupling is realized through the centrosome. Centrosomes are presented as mass particles on the cell poles and represent two rheonomic centers of oscillations. Microtubules could be presented with standard light massless elastic or visco-elastic or fractional order type elements depending on the age of the specific cell. We proposed that mechanical elements that could describe the visco-elastic behavior could be used to model dynamical oscillatory behavior of microtubules in aged cells. In this paper, for the simplicity of the model, microtubules are considered elastic. Homologue chromosomes are represented as mass particles that are interconnected with standard light massless linear elastic spring. Homologue chromosomes have equal masses and different chromosomes have different masses. System is, in static equilibrium in state without force excitation; symmetrical in relation to the horizontal plane like an image in the mirror. Homologue chromosomes are arranged in two symmetric and parallel planes to the equatorial plane. Centrosomes - microtubule

organizing centers generate oscillations and governed movements of microtubules and attached chromosomes in the mitotic spindle [74].



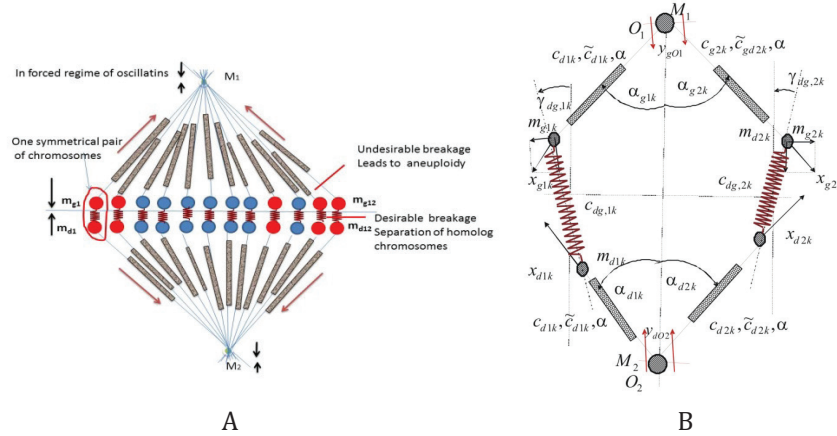A                                                    B

FIGURE 9. A. The biomechanical model of the mitotic spindle in a forced regime of oscillations with different distribution of chromosomes with different masses. Rectangles denote visco-elastic elements that represent microtubules. Elastic springs denote connections between pairs of homologue chromosomes-kinetochore complexes. B. A general oscillatory model of mitotic spindle with inertia elements on the poles of the cell that represents centrosomes. Only two pairs of homologue chromosomes are presented. Kinematical excitation of the mitotic spindle occurs in the centrosomes-rheonomic centers in vertical axis with synchronous or asynchronous kinematic excitation. Taken from [72].

Assumptions of the model: rheonomic centres of oscillation with masses $M_1$ and $M_2$ generate oscillations and oscillate along the vertical axis. Oscillations are transferred trough standard light elastic or visco-elastic elements to homologue chromosomes – the mass particle and its homologue pair. During anaphase A homologue chromosomes are disconnected (elastic spring that interconnects mass particles breaks) and homologues are moving in an oscillatory manner to the corresponding centrosomes-spindle rheonomic oscillatory centres.

For the simplicity of the model we consider that system is conservative without energy dissipation; kinematical excitation of rheonomic centres of oscillations is each with a single frequency and only in the vertical axis, movement of centrosomes in other axis are neglected. The frequency of excitation of rheonomic centres of oscillations in this paper is considered equal. We assume that eigen oscillations of the subsystem are negligible, and is not considered.

### Oscillatory motions of chromosomes

Each pair of homologue chromosomes has two component velocities: a relative velocity ($\dot{x}_{gik}$ and $\dot{x}_{dik}$) in direction of standard light elastic or visco-elastic element and components of transfer velocity: in collinear ($\dot{y}_{gO1}\cos\alpha_{gik}$ and $\dot{y}_{dO1}\cos\alpha_{dik}$) and

in orthogonal ($\dot{y}_{gO1}\sin\alpha_{gik}$ and $\dot{y}_{dO1}\sin\alpha_{dik}$) directions of the standard light elastic or visco-elastic element. Fig. 9B.

The square of absolute velocity of homologue chromosomes in each subset –are: for upper

$$v_{gik}^2 = \left(\dot{x}_{gik}+\dot{y}_{gO1}\cos\alpha_{gik}\right)^2 + \left(\dot{y}_{gO1}\sin\alpha_{gik}\right)^2 \tag{23}$$

and lower:

$$v_{dik}^2 = \left(\dot{x}_{dik}+\dot{y}_{dO2}\cos\alpha_{dik}\right)^2 + \left(\dot{y}_{dO2}\sin\alpha_{dik}\right)^2 \tag{24}$$

sister chromatids in equatorial plain of a mitotic spindle.

$\dot{y}_{gO1}$ and $\dot{y}_{dO2}$ are velocities of kinematic excitation of rheonomic centers with masses $M_1$ and $M_2$.

Approximate value of elongation of a standard light linear elastic element that interconnect pairs of sister chromatids in homologues chromosomes is:

$$\Delta\ell_{ik} \approx -\left[\left(y_{gO1}+y_{dO1}\right)+\left(x_{gik}\sin\alpha_{gik}+x_{dik}\sin\alpha_{dik}\right)\right] \tag{25}$$

## 4.2. Resonance as a potential mechanism for homologue chromosomes separation.

We suggested that the mechanism for homologue chromosome separation in anaphase of mitotic spindle could be the mechanism of resonance. This mechanism can be explained through an oscillatory model of the mitotic spindle using a biomechanical approach. The conditions for resonance as a potential mechanism for homologue chromosomes separation are analysed through a system of $N$ coupled subsystems of ordinary fractional order differential equations that describes motions of the material particles in the system in forced oscillatory regime. If we expressed properties of visco-elastic elements with constitutive relation in fractional order derivatives by generalized function of fractional order dissipation of subsystem energy, we will have a system of fractional order differential equations, obtained by extended Lagrange's differential equations. Considering the coupling of homologue chromosomes in the proposed mechanical oscillatory model of the mitotic spindle, in general case, we will have a system of 20 (for mice) or 24 (for humans) pairs of coupled fractional order differential equations. Each pair of coupled fractional order differential equations could be solved independently from the other coupled pairs of the oscillatory mitotic spindle [72].

For generalized coordinates $x_{gik}$ and $x_{dik}$, we will obtain a system with 20/24 sub-systems, each with one pair of the ordinary fractional order differential equations that, after linearization, has the following form:

$$\ddot{x}_{gik}+\left(\omega_{gik}^2+\widehat{\omega}_{gik}^2\sin^2\alpha_{gik}\right)x_{gik}+\left(\widehat{\omega}_{gik}^2\sin\alpha_{dik}\sin\alpha_{gik}\right)x_{dik}+\tilde{\omega}_{gik}^2 x_{gik}$$
$$=\left(\Omega_g^2 h_{0,gik}-\widehat{\omega}_{gik}^2\tilde{h}_{0,gik}\right)\cos\Omega_g t-\widehat{\omega}_{gik}^2\tilde{\tilde{h}}_{0,gik}\cos\Omega_d t \tag{26}$$

$$\ddot{x}_{dik}+\left(\omega_{dik}^2+\widehat{\omega}_{dik}^2\sin^2\alpha_{dik}\right)x_{dik}+\tilde{\omega}_{dik}^2 x_{gik}-\left(\widehat{\omega}_{dik}^2\sin\alpha_{gik}\sin\alpha_{dik}\right)x_{gik}=$$
$$=\left(\Omega_d^2 h_{0,dik}+\widehat{\omega}_{dik}^2\tilde{h}_{0,dik}\right)\cos\Omega_d t+\widehat{\omega}_{dik}^2\tilde{\tilde{h}}_{0,dik}\cos\Omega_g t \tag{27}$$

where $\omega_{gik}^2 = \dfrac{c_{gik}}{m_{gik}}$ , $\omega_{gik}^2 = \dfrac{c_{gik}}{m_{gik}}$ , $\widetilde{\omega}_{gik}^2 = \dfrac{\widetilde{c}_{gik}}{m_{gik}}$ , $h_{0,gik} = y_{go} \cos \alpha_{gik}$ ,

$\omega_{dik}^2 = \dfrac{c_{dik}}{m_{dik}}$ , $\widetilde{\omega}_{dik}^2 = \dfrac{\widetilde{c}_{dik}}{m_{dik}}$ , $h_{0,dik} = y_{do} \cos \alpha_{dik}$ , $\widehat{\omega}_{gik}^2 = \dfrac{c_{ik}}{m_{gik}}$ , $\widehat{\omega}_{dik}^2 = \dfrac{c_{ik}}{m_{dik}}$ ,

$\widetilde{h}_{0,gik} = y_{g0} \sin \alpha_{gik}$ , $\qquad \widetilde{\widetilde{h}}_{0,gik} = y_{d0} \sin \alpha_{gik}$ , $\qquad \widetilde{h}_{0,dik} = y_{d0} \sin \alpha_{dik}$ ,

$\widetilde{\widetilde{h}}_{0,dik} = y_{g0} \sin \alpha_{dik}$, $\Omega_g$ and $\Omega_d$, are frequencies of forced oscillations of kinematic excitations of centrosomes with masses $M_1$ and $M_2$ amplitudes $y_{g0}$ and $y_{d0}$; $x_{gik}$ and $x_{dik}$ are independent generalized coordinates, $c_{gik}$ , $c_{dik}$ and $c_{ik}$ are rigidities of standard light visco-elastic and elastic elements – coupling between pair of mass particles.

Particular solutions of modified ordinary differential equations (26) and (27) are:

$$x_{Pgik} = D_{gik} \cos \Omega_g t + \widetilde{D}_{gik} \cos \Omega_d t \tag{28}$$

$$x_{Pdik} = D_{dik} \cos \Omega_g t + \widetilde{D}_{dik} \cos \Omega_d t \tag{29}$$

where $D_{gik}$ , $D_{dik}$ , $\widetilde{D}_{gik}$ and $\widetilde{D}_{dik}$ are unknown amplitudes.

When we introduce proposed particular solutions (28) and (29) and their second derivatives into differential equations (26) and (27) we obtain a system of differential equations that could be transformed into a system of coupled non-homogeneous algebraic equations with unknown amplitudes of proposed particular solutions in the following forms:

$$\left[\left(\omega_{gik}^2 + \widehat{\omega}_{gik}^2 \sin^2 \alpha_{gik}\right) - \Omega_g^2\right] D_{gik} + \left(\widehat{\omega}_{gik}^2 \sin \alpha_{dik} \sin \alpha_{gik}\right) D_{dik} = \left(\Omega_g^2 h_{0,gik} - \widehat{\omega}_{gik}^2 \widetilde{h}_{0,gik}\right)$$

$$\left[\left(\omega_{gik}^2 + \widehat{\omega}_{gik}^2 \sin^2 \alpha_{gik}\right) - \Omega_d^2\right] \widetilde{D}_{gik} + \left(\widehat{\omega}_{gik}^2 \sin \alpha_{dik} \sin \alpha_{gik}\right) \widetilde{D}_{dik} = -\widehat{\omega}_{gik}^2 \widetilde{\widetilde{h}}_{0,gik} \tag{30}$$

$$\left[\left(\omega_{dik}^2 + \widehat{\omega}_{dik}^2 \sin^2 \alpha_{dik}\right) - \Omega_g^2\right] D_{dik} + \left(\widehat{\omega}_{dik}^2 \sin \alpha_{gik} \sin \alpha_{dik}\right) D_{gik} = \widehat{\omega}_{dik}^2 \widetilde{h}_{0,dik}$$

$$\left[\left(\omega_{dik}^2 + \widehat{\omega}_{dik}^2 \sin^2 \alpha_{dik}\right) - \Omega_d^2\right] \widetilde{D}_{dik} + \left(\widehat{\omega}_{dik}^2 \sin \alpha_{gik} \sin \alpha_{dik}\right) \widetilde{D}_{gik} = \left(\Omega_d^2 h_{0,dik} + \widehat{\omega}_{dik}^2 \widetilde{\widetilde{h}}_{0,dik}\right) \tag{31}$$

This coupled system could be further decoupled into two independent subsystems (30) and (31). Finding the determinant and sub-determinants of each of the systems, we can find the unknown amplitudes:

$$x_{Pgik} = D_{gik} \cos \Omega_g t + \widetilde{D}_{gik} \cos \Omega_d t = \frac{\Delta_{1,ik}}{\Delta_{ik}} \cos \Omega_g t + \frac{\widetilde{\Delta}_{1,ik}}{\widetilde{\Delta}_{ik}} \cos \Omega_d t \tag{32}$$

$$x_{Pdik} = D_{dik} \cos \Omega_g t + \widetilde{D}_{dik} \cos \Omega_d t = \frac{\Delta_{2,ik}}{\Delta_{ik}} \cos \Omega_g t + \frac{\widetilde{\Delta}_{2,ik}}{\widetilde{\Delta}_{ik}} \cos \Omega_d t \tag{33}$$

Where $\Delta_{ik}$ and $\widetilde{\Delta}_{ik}$ are determinants of the systems (30) and (31) respectively and $\Delta_{1,ik}$ , $\Delta_{2,ik}$ , $\widetilde{\Delta}_{1,ik}$ and $\widetilde{\Delta}_{2,ik}$ are sub-determinants. When the determinant of one system is $\Delta_{ik} = 0$ or $\widetilde{\Delta}_{ik} = 0$, we can obtain resonant frequencies of kinematic excitation of rheonomic centres. When one of the amplitudes $D_{gik} = \dfrac{\Delta_{1,ik}}{\Delta_{ik}} = 0$

or $D_{dik} = \dfrac{\Delta_{2,ik}}{\Delta_{ik}} = 0$ or $\tilde{D}_{gik} = \dfrac{\tilde{\Delta}_{1,ik}}{\tilde{\Delta}_{ik}} = 0$ or $\tilde{D}_{dik} = \dfrac{\tilde{\Delta}_{2,ik}}{\tilde{\Delta}_{ik}} = 0$ is equal to zero, or determinants $\Delta_{1,ik} = 0$ and $\Delta_{2,ik} = 0$ or/and $\tilde{\Delta}_{1,ik} = 0$, $\tilde{\Delta}_{2,ik} = 0$, dynamical absorption of corresponding amplitude, forced mode and force frequency, in corresponding homologue chromosome occurs.

From the theory of oscillations, dynamic absorption could be the explanation why some pairs of homologue chromosomes postpone their movements until other pairs of homologues are not in the right position in equatorial plain.

"If dilatation $\left(\Delta \ell_{ik}\right)_{critical}$ according to the (25) reaches, in resonant state, critical value for disconnection of pair of homologue chromosomes-material particles before the critical value of breakage of opposite microtubules-both dilatations $\left(x_{Pgik}\right)_{critical}$ and $\left(x_{Pdik}\right)_{critical}$ is reached, homologue chromosomes are separated and move to the corresponding centrosome. In the case when one of the dilatations $\left(x_{Pdik}\right)_{critical}$ or $\left(x_{Pdik}\right)_{critical}$ reaches the critical value of breakage, in resonant state, before $\left(\Delta \ell_{ik}\right)_{critical}$ is reached, aneuploidia occurs and an aberrant spindle assembly-an undesirable and unfavourable state for equal distribution of genetic material in sister cells. Which of these scenarios will occur depends on resonant frequencies of excitation of rheonomic centers, angles between microtubules (standard light visco-elastic element) and centrosome (rheonomic center of excitation) as well as of rigidities and chromosomal masses in oscillatory system of mitotic spindle"[72].

As aging causes a loss of meiotic chromosome cohesion, which can explain premature disjunction of sister chromatids [75] the proposed model could be suitable for explaining age related aberrations in the mitotic spindle.

Using the previously developed methodology [72, 76] and data from the literature the resonant frequencies of mouse chromosomes were analyzed [77, 78]. Resonant frequencies curves for first 10 mouse chromosomes are presented on Fig 10, 11, and 12.

For each homologue chromosome pair, we obtained non-linear frequency curves and identified two eigen resonant frequencies that behave differently [78]. First resonant frequency is almost the same for all pairs of homologue chromosomes (Fig. 11), while the second resonant frequency increases as the mass of a homologue chromosome decreases (Fig 12). First, lowest eigen frequency of each pair of two mass in an oscillator with two degrees of freedom, is the same as frequency of the corresponding oscillator built with one degree of freedom, caused by model with symmetry. The first resonant frequency is impacted by the chromosome masses which are very similar to each other, while the second resonant frequency is impacted both by the chromosome mass and its position in the mitotic spindle. The findings are important for understanding the process of cell division.

Impact of centrosome frequency [79] and spindle size [80] on potential [81]and kinetic energy [82] of sister chromatids were also analysed using the g oscillatory model of a mitotic spindle.
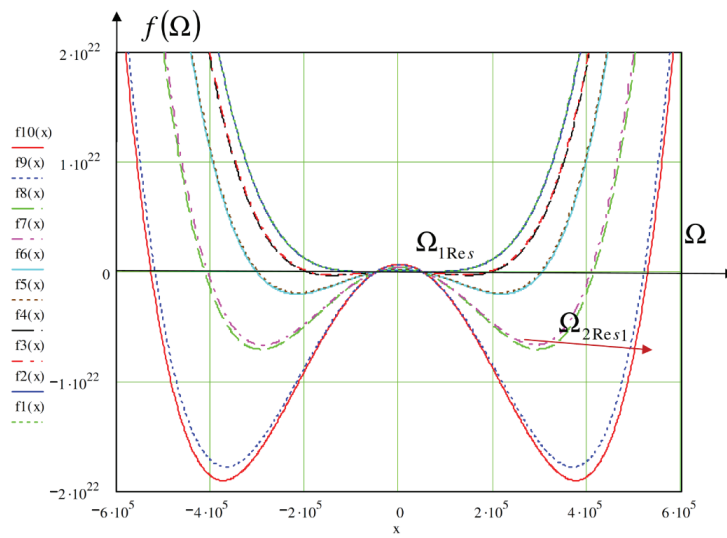
FIGURE 10. Frequency curve for first 10 mouse chromosomes. Only the right part of the curve has mechanical sense-positive values of resonant frequencies.
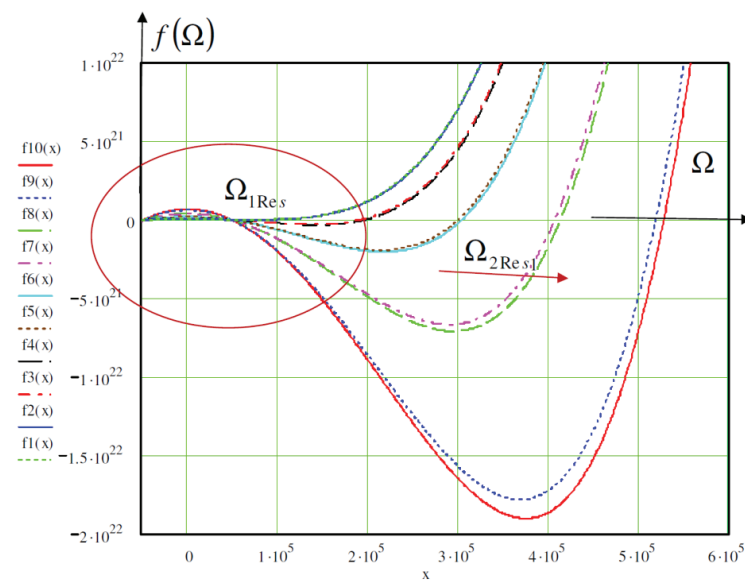


FIGURE 11. A detail from Fig 10. First resonant frequency is almost equal for all 10 mouse chromosomes.
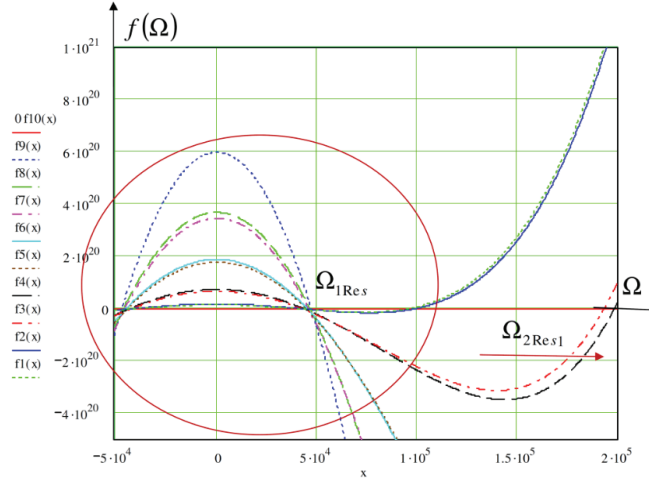
FIGURE 12. A detail from Fig 10: The second resonant frequency increases as mass of a homologue chromosome decreases.

Total kinetic energy $\mathbf{E}_{K,ik}$ of $ik$-pair of homologue chromosomes including kinetic energies of centrosome caused by rheonomic excitation coupled with a standard light elastic element under angle $\alpha_{gik} = \alpha_{dik} = \alpha_{ik}$ with direction of kinematic excitation is:

$$\mathbf{E}_{K,ik} = \frac{1}{2}m_{gik}\left[(\dot{x}_{gik} + \dot{y}_{gO1}\cos\alpha_{gik})^2 + (\dot{y}_{gO1}\sin\alpha_{gik})^2\right] + \frac{1}{2}m_{dik}\left[(\dot{x}_{dik} + \dot{y}_{dO2}\cos\alpha_{dik})^2 + (\dot{y}_{dO2}\sin\alpha_{dik})^2\right] +$$
$$+ \frac{1}{2}M_{3}\dot{y}_{gO1}^2 + \frac{1}{2}M_{3}\dot{y}_{gO2}^2 \tag{34}$$

with assumption that rheonomic centres of excitations are equal.

Expression of potential energy $\mathbf{E}_P$ of two standard visco-elastic and one standard light elastic element contained in each of the sub-systems with one pair of coupled two mass particles and rheonomic centre is:

$$\mathbf{E}_P = \mathbf{E}_{P,gik} + \mathbf{E}_{P,dik} + \mathbf{E}_{PE,ik}$$
$$\mathbf{E}_P = \frac{1}{2}c_{gik}x_{gik}^2 + \frac{1}{2}c_{dik}x_{dik}^2 + \frac{1}{2}c_{ik}\left[(y_{gO1} + y_{dO2}) + (x_{gik}\sin\alpha_{gik} + x_{dik}\sin\alpha_{dik})\right]^2 \tag{35}$$

with assumption that rheonomic centres of excitations are equal. See ref [72].

## 4.3. Distribution of mechanical energies in a mitotic spindle regarding mass distribution.
One of the models that explains the organization of chromosomes during mitosis predicts a central location of gene rich chromosomes within a cell nucleus and gene-poor chromosomes located in a zone close to the nuclear edge [64, 83]. Distribution of chromosomes in equatorial plane of the mitotic spindle, chromosome territories (CT) [84]

and dynamics of chromosome movements towards centrosomes could carry additional epigenetic information.

Regarding the distribution of chromosomes in the equatorial plane of a mitotic spindle and its impact on mitotic spindle dynamics, especially oscillatory movements of homologue chromosomes towards the corresponding centrosome, we analysed how different distributions of homologue chromosome masses in the equatorial plane during metaphase influence the distribution of kinetic and potential energy in the system of the mitotic spindle [85]. For numerical analysis we considered two cases: 1. when homologue chromosomes with heavier masses are located in the central zone of the metaphase equatorial plane, and 2. when homologue chromosomes with heavier masses are located in the peripheral zone of the metaphase plane. See Fig 13. In Fig. 13, a basic model is presented in which microtubules are represented with standard light visco-elastic elements, but for numerical analysis we consider microtubules elastic and represent them with a standard light elastic element. Numerical analyses were done for mouse chromosome masses. A mouse has 20 pairs of chromosomes. The angle of a mitotic spindle-an angle between rheonomic centers and the chromosomes on the very periphery of the mitotic spindle was taken to be $\pi/2$. Regarding the vertical axis that interconnects two opposite rheonomic centres- centrosomes, homologue chromosomes are equally distributed. See Fig. 14.



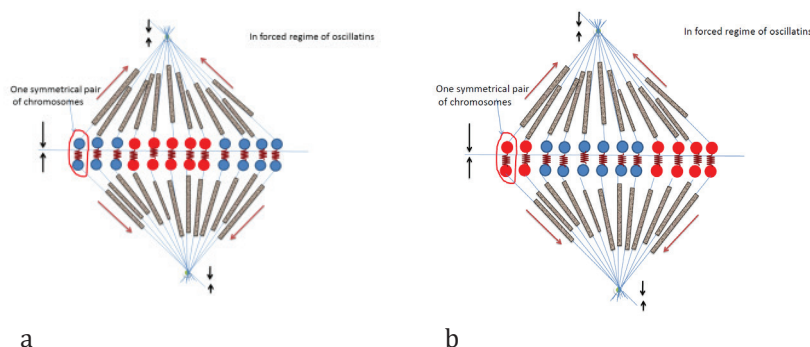a                                                b

Figure 13. The Biomechanical model of the mitotic spindle in forced regime of oscillations with different distributions of chromosomes and the different masses-symmetrical distribution of chromosomes mass in the mitotic spindle. a) Heavy chromosomes are in a central position. b) Heavy chromosomes are in a peripheral position. Rectangles denote visco-elastic elements that represent microtubules. Elastic springs denote connections between pairs of homologue chromosomes.

Data for chromosomal mass for mouse chromosomes were taken from ref [86]. As data in the ref [86] denotes masses for 4 chromatids data from the table from ref [86] were divided with 2 and expressed in pg. Data for rigidity of eukaryote metaphase chromosomes was taken from [87] -1kPa=$10^3$ pN/$\mu$m$^2$. Rigidity for microtubules at 37° C were taken from ref [88] ($1.9 \times 10^{11}$ pN/$\mu$m$^2$). Data for rheonomic centers of oscillation was calculated according to the data for angular frequency oscillation for

centrosome were taken from [89] (2π/T, T=20s). Centrosome mass was calculated from centrosome volume (1,5μm³) from http://www.proteinatlas.org/humancell/centrosome and density - (density was taken approximatively as data for density for cell organelle- mitochondria 1,05g/ml) – (1.575pg) [90]. Data for centrosome amplitude oscillations was taken from [91] (2.1μm).

Total mechanical energy for each pair of homologue chromosomes subsystem for the case when heavy chromosomes take a central position in the mitotic spindle are presented in Fig 15. From the graph it is evident that amplitudes of total energy for each pair of homologue chromosomes subsystem have lower values in the central zone of mitotic spindle compare to the amplitudes of total mechanical energy for each pair of homologue chromosomes positioned at the periphery of the mitotic spindle.
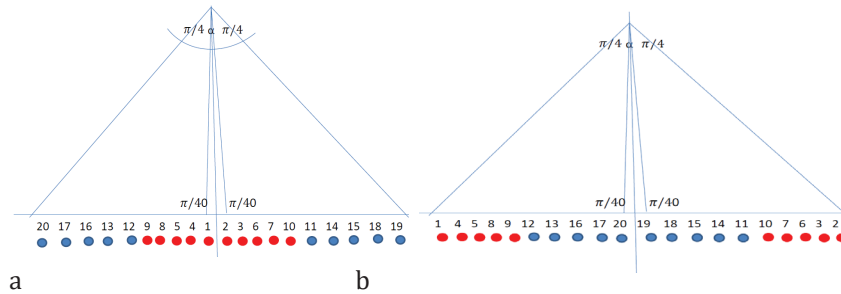


FIGURE 14. Schematic representation of the potential distribution of mouse mitotic chromosomes in equatorial plane in metaphase used for numerical modeling with a biomechanical model of mitotic spindle-half section. A. The case when chromosomes with heavier masses are in the central part of the mitotic spindle. B. Case when chromosomes with heavier masses are in the peripheral part of the mitotic spindle. Angle of mitotic spindle was taken to be π/2, angles between centrosome - rheonomic center of oscillations and direction of microtubules - elastic element are assumed to equally increase from the central to the peripheral zone of the mitotic spindle (for π/4). The distribution of chromosome masses are assumed to be relatively symmetrically distributed in relation to the symmetry line that interconnects two rheonomic centers (intercentromeres' distance). The model has a relatively balanced distribution of chromosomal masses in the vertical axis of symmetry, and an identical distribution of masses in the horizontal plane - homologue chromosomes.

The distribution of the total mechanical energy of each chromosome pair for the case when chromosomes with heavier masses are positioned in the peripheral part of the equatorial plane are presented on Fig. 16. In this case amplitudes of the total mechanical energy for each pair of homologue chromosomes have also lower values in the central zone of mitotic spindle compared to the amplitudes of total mechanical energy for each pair of homologue chromosomes positioned at the periphery of the mitotic spindle but values of amplitudes are higher compared to the first case when chromosomes with heavier masses are positioned in the central part of the mitotic spindle. Kinetic and

potential energy for each dyad of sister chromatids follow the same pattern [81, 92]. If this biomechanical system follows the minimum energy principle for its stability, than the system of mitotic spindle will be more stable in the case when chromosomes with heavier masses are positioned in the central zone of the metaphase plate.
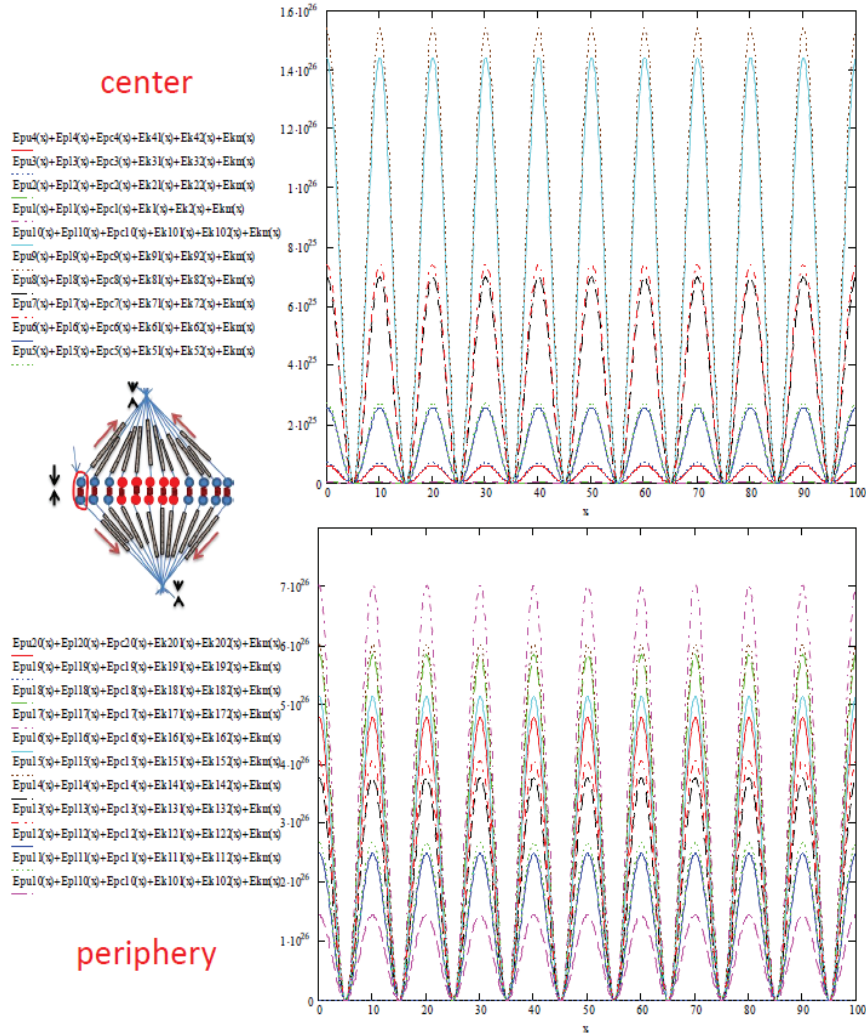


FIGURE 15. The distribution of total energy of each chromosome pair for the case when chromosomes with higher masses are positioned in the central part of the equatorial plane. Lower values of energy of each pair of homologue chromosomes are arranged in the central part of the biomechanical model of the mitotic spindle (upper diagram). Energy expressed in $\frac{pg \cdot \mu m^2}{s^2}$ is shown on the vertical axis. On the horizontal axis (x) is time in seconds (s).
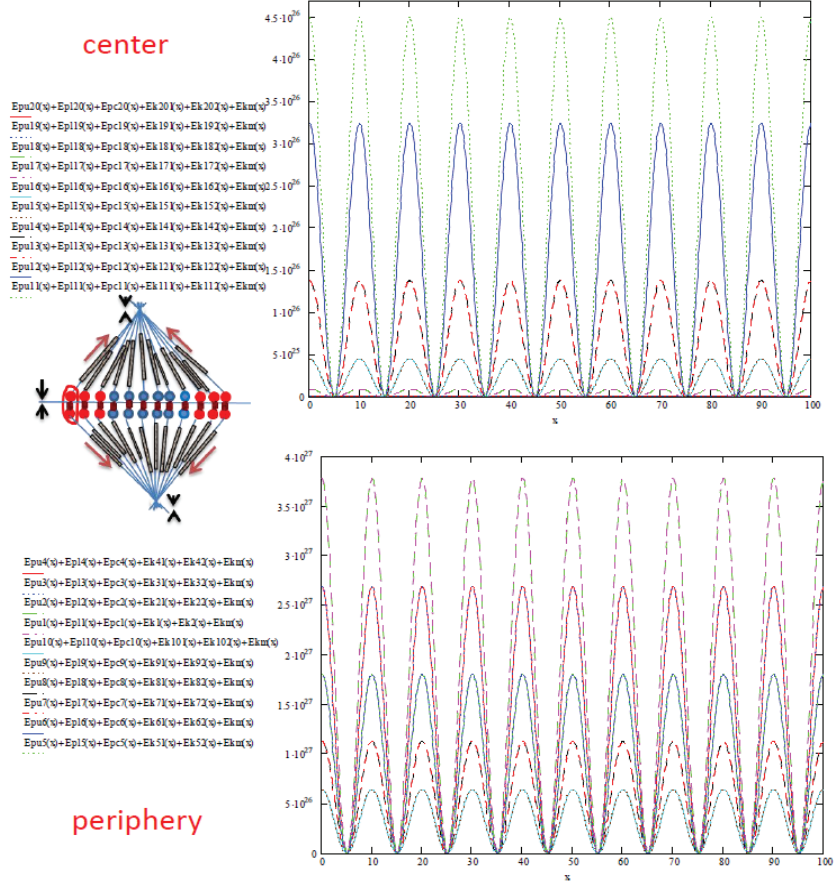
FIGURE 16. The distribution of the total energy of each chromosome pair for the case when chromosomes with higher masses are positioned in the peripheral part of the equatorial plane. Lower values of energy of each pair of homologue chromosomes are arranged in the central part of the biomechanical model of the mitotic spindle (upper diagram). Energy expressed in $\frac{pg \cdot \mu m^2}{s^2}$ is shown on the vertical axis. On the horizontal axis (x) is time in seconds (s).

The mass distribution of chromosomes in equatorial plane in static equilibrium position, in dynamical oscillatory state and forced regimes influences the distribution of potential, kinetic and total mechanical energy for each pair of homologue chromosome subsystems in the system of oscillatory mitotic spindle. Regardless of the distribution of chromosome masses (central or peripheral position of chromosomes with heavier masses) kinetic, potential and total mechanical energy for each particular pair of homologue chromosomes are lower in the central zone of the mitotic spindle, but amplitudes of kinetic, potential and total mechanical energy for each pair of homologue chromosomes subsystems are lower when chromosomes with heavier masses are positioned in the central zone of the mitotic

spindle compared to the case when they have peripheral positions in the mitotic spindle. The results we obtain by numerical analysis could be explained by non-linear dependence of the angle between microtubule (elastic element) and centrosome-rheonomic centre. This difference in energy distribution could be of importance for the stability of the system of the mitotic spindle and its energy balance. Also this difference in energy distribution during metaphase may carry additional epigenetic information and could be important for the process of differentiation.

We must point out, that all numerical analysis are conducted for the conservative model without energy dissipation and for a forced oscillatory regime when rheonomic centres are excited by a single frequency. In the considered case, we assume that eigen vibrations of the subsystem are negligible, and it is not taken into calculations.

Elements that represent microtubules in the oscillatory model of mitotic spindle can be modelled as visco-elastic elements. Fig 16. In that case, fractional calculus can be used for modelling energy dissipation of the system.

## 4.4. The fractional order oscillatory model of the mitotic spindle. The
fractional order oscillatory model of the mitotic spindle is presented in [77, 93]. Fig 17. This concept was used because elastic properties of microtubules could change in aging cells. We postulate that microtubules lose elasticity when the cell ages.
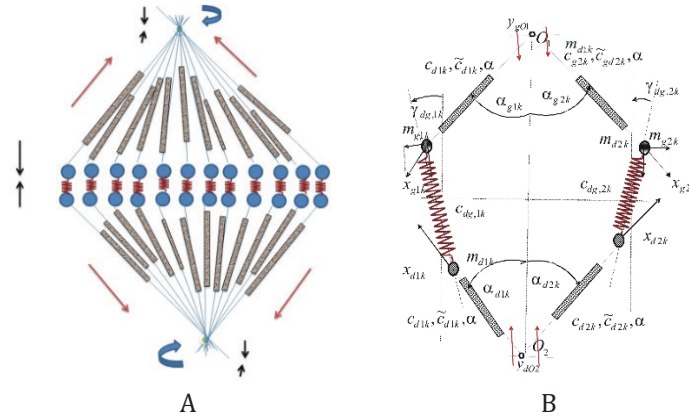


FIGURE 17. The biomechanical oscillatory model of the mitotic spindle with microtubules as visco-elastic elements. 1A. case when chromosomes are arranged in equatorial plane. 1B. part of the model with only two chromosomes. Beads represent chromosomes with a certain mass $m$, rectangles represent standard light fractional order elements (SLFE) that have visco-elastic properties and denote microtubules. $O_1$ and $O_2$ are autonomous oscillatory centres. $\alpha_{d,ik}$ or $\alpha_{d,ik}$ is an angle between direction of SLFE and source of oscillations, $c_{gik}$, $\widetilde{c}_{gik}$ or $c_{dik}$, $\widetilde{c}_{dik}$ are linear rigidity and fractional order coefficients for SLFE. $x_{gik}$ or $x_{dik}$ -coordinates of relative displacements of chromosomes, $y_{gO1}(t)$ or $y_{dO2}$–rheonomic coordinates of displacements of oscillatory centres $O_1$ and $O_2$, kinematically excited. Arrow denotes directions of motions. Taken from [94].

**Mechanical energies and the generalized function of fractional order dissipation of energy of biomechanical model.** Expressions of the total kinetic energy of the proposed biomechanical system, presented in Fig. 17B. is:

$$\mathbf{E}_K = \frac{1}{2}\sum_{k=1}^{k=N}\sum_{i=1}^{i=2} m_{gik}\left[\left(\dot{x}_{gik}+\dot{y}_{gO1^2}\cos\alpha_{gik}\right)^2+\left(\dot{y}_{gO1}\sin\alpha_{gik}\right)^2\right]+\frac{1}{2}\sum_{k=1}^{k=N}\sum_{i=1}^{i=2} mn_{dik}\left[\left(\dot{x}_{dik}+\dot{y}_{dO1^2}\cos\alpha_{dik}\right)^2+\left(\dot{y}_{dO1}\sin\alpha_{dik}\right)^2\right] \qquad (36)$$

where expressions under square denote the square of the absolute velocity of one chromosome/ $k$ -th material particle-chromosome.

The expression of potential energy of the chromosome displacements along axial deformation of the standard light fractional order element is:

$$\mathbf{E}_P = \sum_{k=1}^{k=N}\sum_{i=1}^{i=2}\mathbf{E}_{P,gik} + \sum_{k=1}^{k=N}\sum_{i=1}^{i=2}\mathbf{E}_{P,dik} = \frac{1}{2}\sum_{k=1}^{k=N}\sum_{i=1}^{i=2} c_{gik}x_{gik}^2 + \frac{1}{2}\sum_{k=1}^{k=N}\sum_{i=1}^{i=2} c_{dik}x_{dik}^2 \qquad (37)$$

Expression of potential energy of the standard light linear elastic element interconnecting two mass particles/homologues chromosomes in one pair, taking into account approximate values of elongation of standard light linear elastic element that interconnect pairs of homologues chromosomes, is in the following form:

$$\mathbf{E}_{PE} \approx \frac{1}{2}\sum_{k=1}^{k=N}\sum_{i=1}^{i=2} c_{ik}\left\langle\left[\left(y_{gO1}+y_{dO1}\right)+\left(x_{gik}\sin\alpha_{gik}+x_{dik}\sin\alpha_{dik}\right)\right]\right\rangle^2 \qquad (38)$$

The expression of the generalized function of the fraction order dissipation of the biomechanical model system energy is:

$$\mathbf{P}_W = \sum_{k=1}^{k=N}\sum_{i=1}^{i=2}\mathbf{P}_{W,gik} + \sum_{k=1}^{k=N}\sum_{i=1}^{i=2}\mathbf{P}_{W,dik} = \frac{1}{2}\sum_{k=1}^{k=N}\sum_{i=1}^{i=2}\widetilde{c}_{gik}\left(\mathbf{D}_t^\alpha\left[x_{gik}\right]\right)^2 + \frac{1}{2}\sum_{k=1}^{k=N}\sum_{i=1}^{i=2}\widetilde{c}_{dik}\left(\mathbf{D}_t^\alpha\left[x_{dik}\right]\right)^2 \qquad (39)$$

where $\mathbf{D}$ is the fractional order $\alpha$ differential operator of the Louisville type [77].

The dynamics of each pair of homologue chromosomes can be modelled as a pair of coupled ordinary fractional order differential equations that can be solved independently. Using the Laplace transformation and the development into a series [94], analytical approximate solutions of coupled ordinary fractional order differential equations for forced vibration regimes are determined [93]. Eigen main coordinates and eigen main fractional order modes for forced vibrations of the considered fractional type oscillatory model are determined in an analytical form. The analytical solution revealed that fractional type main modes for forced regimes are independent, that there are no interactions and energy transfers between modes, but that total mechanical energies of modes are not constant. System behaviour is linear [93]. The model is suitable for explaining mitotic spindle disorders in a context of numerical chromosomal aberrations and the oscillatory behaviour of chromosomes in the mitotic spindle in young and aged cells [77]. During the process of ageing chromatin structure will be modified in different ways [95]. Microtubules exhibit dynamical instability in the mitotic spindle during the process of cell division, but their dynamics will be also affected by the ageing process [96, 97]. To model the dynamical behaviour of a mitotic spindle during metaphase and anaphase that could cover ageing changes in the mitotic spindle constitutive elements, we modified the previously proposed oscillatory model of the mitotic spindle [82].

**Main eigen independent modes for forced vibrations of elements of the mitotic spindle.** Standard light fractional order creep elements and fractional order derivatives of Louisville type were used in the analysis to express constitutive stress-strain relations for the restitution forces as a function of element elongation [94]. Approximate solution in analytical form for that fractional type model is determined and presented in [93]. A general solution for fractional order forced modes is:

$$\xi_s\left(t,\alpha,\omega_s,\omega_{(\alpha)s},\Omega_1,\Omega_2\right)=\xi_s\left(t,\alpha,\omega_s,\omega_{(\alpha)s}\right)+\xi_{s,p,\cos}\left(t,\alpha,\omega_s,\omega_{(\alpha)s},\Omega_1,\Omega_2\right)=$$

$$+\overline{\xi}_s(0)\sum_{k=0}^{\infty}(-1)^k\omega_{(\alpha)s}^{2k}t^{2k}\sum_{j=0}^{k}\binom{k}{j}\frac{(\mp1)^j\omega_{(\alpha)s}^{-2j}t^{-\alpha j}}{\omega_s^{2j}\Gamma(2k+1-\alpha j)}+$$

$$+\overline{\dot{\xi}}_s(0)\sum_{k=0}^{\infty}(-1)^k\omega_{(\alpha)s}^{2k}t^{2k+1}\sum_{j=0}^{k}\binom{k}{j}\frac{(\mp1)^j\omega_{(\alpha)s}^{-2j}t^{-\alpha j}}{\omega_s^{2j}\Gamma(2k+2-\alpha j)}+$$

$$+\int_0^t\Big\langle h_{s1}\cos n(\Omega_1(t-\tau)+h_{s2}\cos(\Omega_w(t-\tau)))\Big\langle\sum_{k=0}^{\infty}(-1)^k\omega_{(\alpha)s}^{2k}\tau^{2k+1}\sum_{m=0}^{k}\binom{k}{m}\frac{\omega_{(\alpha)s}^{-2m}\tau^{-\alpha m}}{\omega_s^{2m}\Gamma(2k+2-\alpha m)}\Big\rangle d\tau-$$

$$-\int_0^t\Big\langle\Big\langle h_{(\alpha)s}\,\mathfrak{D}_\alpha^t\big[\big(h_{0,dik}\cos\Omega_g(t-\tau)+\widetilde{h}_{0,dik}\cos\Omega_d(t-\tau)\big)\big]\Big\rangle\Big\langle\sum_{k=0}^{\infty}(-1)^k\omega_{(\alpha)s}^{2k}\tau^{2k+1}\sum_{m=0}^{k}\binom{k}{m}\frac{\omega_{(\alpha)s}^{-2m}\tau^{-\alpha m}}{\omega_s^{2m}\Gamma(2k+2-\alpha m)}\Big\rangle d\tau$$

$$s=1,2 \tag{40}$$

Fractional type main modes for forced regimes are independent, there are no interactions and no energy transfer between modes, but total mechanical energies of modes are not constant. System behavior is linear [93].

## 4.5. Relation between centrosome excitation and oscillatory energy of a mitotic spindle. 
Orientation of the mitotic spindle and the position of the centrosome affects polarity and function of new cells [66, 98, 99]. Polarity of the cells plays a great role in cell differentiation.

The relation between centrosome excitation and oscillatory energy of mitotic spindle is studied in [79, 92, 100]. "Our results show that centrosome frequency change can change energy of the same homologue pair of chromosomes when it remains in the same position in the mitotic spindle indicating that centrosome frequency change can change energy code of the chromosome pair. Changing the frequency of centrosome oscillations induces a phase shift in kinetic and potential energy curves of the same oscillating homologue chromosome pair. Besides, kinetic energy of the same chromosome pair shows amplitude change with centrosome frequency change. This could be of importance for the process of cell differentiation." [79].

Narrow and long mitotic spindles as well as wide and short are indicative of some mitotic spindle disorders typical for old or cancerous cells. It will be of interest to study the influence of width of the mitotic spindle on the energy distribution in the system of the mitotic spindle using this biomechanical oscillatory model.

Also, centrosomes – rheonomic centres in real biological system could have different frequencies as well as different amplitudes of oscillations that will have influence on amplitudes of energy of oscillations for each pair. "Spindle size affects

total mechanical energy of each homologue chromosome pair. Total mechanical energy for each homologue chromosome pair increases with mitotic spindle size-angle. This approach could be useful for understanding mitotic spindle size disorders" [80].

"If centrosomes oscillate with different frequencies, the energy of dyads of sister chromatids has a non-linear oscillatory character. The maximum values of the amplitudes of the kinetic energy of the same dyad are equal in the case of equal frequencies of forced centrosome excitation"[92].

## 5. Conclusion

Three different mechanical models of biological oscillators were presented: the oscillatory model of double DNA helix, the spherical oscillatory net model of mouse ZP and the oscillatory model of the mitotic spindle. The models have different levels of complexity and are suitable for explaining some biological phenomena like: unfolding the double DNA helix in the process of transcription, conditions for initiation of transcription, sperm penetration trough ZP of the oocyte as a result of resonance phenomenon, separation of sister chromatids in anaphase of cell division cycle as a result of resonance. We also postulate that the energy of moving chromosomes within the cell during the cell division cycle could be an important physical parameter for epigenetic coding. It could be of great importance for explaining the process of cell differentiations but also of cancerogenesis. The concept and the theory of the oscillatory model of mitotic spindle could open new possibilities for cancer treatment.

### Acknowledgement

## References

[1]   A. N. Hedrih, *Mechanical models of the double DNA*, Int. J. Med. Eng. Inform. **3**(4) (2011), 394–410. https://doi.org/10.1504/IJMEI.2011.044753.

[2]   H. Shroff, D. Sivak, J. J. Siegel, A. L. McEvoy, M. Siu, A. Spakowitz, P. L. Geissler, J. Liphardt, *Optical measurement of mechanical forces inside short DNA loops*, Biophys. J. **94**(6) (2008), 2179–2186. https://doi.org/10.1529/biophysj.107.114413.

[3]   H. Dalir, Y. Yanagida, T. Hatsuzawa, *Probing DNA mechanical characteristics by dielectrophoresis*, Sensors Actuators, B Chem. **136**(2) (2009), 472–478. https://doi.org/10.1016/j.snb.2008.11.004.

[4]   J. L. D. S. Carlos Bustamante, S. B Smith, *Single-molecule studies of DNA mechanics*, Curr. Opin. Struct. Biol. **10**(2000), 279–285.

[5]   K. R. (Stevanović) Hedrih, A. N. Hedrih, *Transfer of energy of oscillations through the double DNA chain helix*, In: 7th EUROMECH Solid Mechanics Conference, Lisbon, Portugal, September 7-11, 2009, MS-24, Kinetics, Control and Vibrorheology KINCONVI*B*, (2009), 121–135.

[6]   K. R. (Stevanović) Hedrih, A. N. Hedrih, *Eigen modes of the double DNA chain helix vibrations*, J. Theor. Appl. Mech. **48**(1) (2010), 219–231.

[7]   A. N. Hedrih, K. R. (Stevanović) Hedrih, *Modeling double dna helix main chains forced vibrations*, In: Proceedings, Third Serbian (28th Yu) Congress on Theoretical and Applied Mechanics, Vlasina lake, Serbia, 1147–1180, Serbian Society of Mechanics, Vlasina lake, 2011.

[8] K. R. (Stevanović) Hedrih, A. N. Hedrih, *Considering Vibrations of the Double DNA Main Chains Via a Model with Hereditary Properties*, In: IFAC Ohrid 2009. A Preprints Volume from the 6th IFAC Workshop DECOM-09, Ohrid, Republic of Macedonia*, 341–346, The international federation of automatic control by The Society for Electronics, Telecommunications, Automation, and Informatics (ETAI), Macedonian NMO to the IFAC Skopje, 2009.

[9] L. Kovaleva, L. Manevich, *Localized nonlinear oscillation of DNA molecule.*, In: Proceedings of 8th Conference on Dinamical Systems Theory and Applications, 12–15 December, Lodz, Poland, 103–110, Department for Automatic and Biomechanics, Lodz, Poland, 2005.

[10] N. Kovaleva, L. Manevich, V. Smirnov, *Analitical study of coarse-grained model of DNA*, In: Proceedings of 9th Conference on Dinamical Systems Theory and Applications, 17–20 December, Lodz, Poland, 901–908, Department for Automatic and Biomechanics, Lodz, Poland, 2007.

[11] K. R. (Stevanović) Hedrih, A. N. Hedrih, *Phenomenological mapping and dynamical absorptions in chain systems with multiple degrees of freedom*, J. Vib. Control **22**(1) (2016), 18–36. https://doi.org/10.1177/1077546314525984.

[12] K. R. (Stevanović) Hedrih, A. N. Hedrih, *Considering vibrations of the double dna main chains by using two models : hereditary and fractional order model*, In: 10th Conference on dynamical systems-theory and applications, J.M. A. Awrejcewicz, M. Kazmierczak, P. Olejnik, (eds), 829–838, Department for Automatic and Biomechanics, Lodz, Poland, December 7-10, 2009. Łódź, Poland, 2009.

[13] A. N. Hedrih, K. R. (Stevanović) Hedrih, *Modeling Double DNA Helix Main Chains of the Free and Forced Fractional Order Vibrations*, In: Adv. Top. Appl. Fract. Calc. Control Probl. Syst. Stab. Model., N.M. Lazarevic, (ed.), WSEAS Press, 2014, 145–183.

[14] A. N. Hedrih, S. Najman, V. Hedrih, O. Milosevic-Djordjevic, *Structure of relations between the frequency of micronuclei in peripheral blood lymphocytes and age, gender, smoking habits and socio-demographic factors in south-east region of Serbia*, Facta Univ. Ser. Med. Biol., **20**(2) (2018), 47–54. https://doi.org/10.22190/fumb180102008h.

[15] K. R. (Stevanović) Hedrih, A. N. Hedrih, *Eigen modes of the double DNA chain helix vibrations*, J. Theor. Appl. Mech. **48**(1) (2010), 219–231.

[16] A. Hedrih, *Modeling oscillations of zona pelucida before and after fertilization EUROMECH Newsletter, Young Scientist Prize Paper.*, EUROMECH Newsl. **40**(2011), 6–14. https://doi.org/10.1016/S1474-4422(12)70032-7.

[17] A. N. Hedrih, *Осцилаторно понашање Zona-е Pelucida-е миша пре и после оплодње*, PhD Thesis, University of Belgrade, Belgrade, 2016. (in Serbian)

[18] A. N. Hedrih, K. R. (Stevanović) Hedrih, B. Bugarski, *Oscillatory Spherical Net Model of Mouse Zona Pellucida*, J. Appl. Math. Bioinforma. **3**(4) (2013), 225–268.

[19] D. P. L. Green, *Three-dimensional structure of the zona pellucida*, Rev. Reprod. **2**(3) (1997), 147–156. https://doi.org/10.1530/ror.0.0020147.

[20] H. W. Michelmann, D. Rath, E. Töpfer-Petersen, P. Schwartz, *Structural and functional events on the porcine zona pellucida during maturation, fertilization and embryonic development: A scanning electron microscopy analysis*, Reprod. Domest. Anim. **42**(6) (2007), 594–602. https://doi.org/10.1111/j.1439-0531.2006.00829.x.

[21] A. Boccaccio, M. C. Frassanito, L. Lamberti, R. Brunelli, G. Maulucci, M. Monaci, M. Papi, C. Pappalettere, T. Parasassi, L. Sylla, F. Ursini, M. De Spirito, *Nanoscale characterization of the biomechanical hardening of bovine zona pellucida.*, J. R. Soc. Interface **9**(76) (2012), 2871–82. https://doi.org/10.1098/rsif.2012.0269.

[22] M. Papi, R. Brunelli, G. Familiari, M. C. Frassanito, L. Lamberti, G. Maulucci, M. Monaci, C. Pappalettere, T. Parasassi, M. Relucenti, L. Sylla, F. Ursini, M. de Spirito, *Whole-Depth Change in Bovine Zona Pellucida Biomechanics after Fertilization: How Relevant in Hindering Polyspermy?*, PLoS One **7**(9) (2012),. https://doi.org/10.1371/journal.pone.0045696.

[23] G. Familiari, M. Relucenti, R. Heyn, G. Micara, S. Correr, *Three-dimensional structure of the zona pellucida at ovulation*, Microsc. Res. Tech. **69**(6) (2006), 415–426. https://doi.org/10.1002/jemt.20301.

[24] K. R. (Stevanović) Hedrih, *Discrete Continuum Method*, In: Proceedings of Recent Advances in Analytical Dynamics Control, Stability and Differential Geometry, V. Djordjević, (ed.), 30–57, Mathematical institute SANU, Belgrade, Serbia, 2002.

[25] M. Khalilian, M. Navidbakhsh, M. R. Valojerdi, M. Chizari, P. E. Yazdi, *Estimating Young's modulus of zona pellucida by micropipette aspiration in combination with theoretical models of ovum.*, J. R. Soc. Interface **7**(45) (2010), 687–94. https://doi.org/10.1098/rsif.2009.0380.

[26] P. M. Wassarman, *Zona pellucida glycoproteins*, J. Biol. Chem. **283**(36) (2008), 24285–24289. https://doi.org/10.1074/jbc.R800027200.

[27] Y. Murayama, J. Mizuno, H. Kamakura, Y. Fueta, H. Nakamura, K. Akaishi, K. Anzai, A. Watanabe, H. Inui, S. Omata, *Mouse zona pellucida dynamically changes its elasticity during oocyte maturation, fertilization and early embryo development.*, Hum. cell  Off. J. Hum. Cell Res. Soc. **19**(4) (2006), 119–125. https://doi.org/10.1111/j.1749-0774.2006.00019.x.

[28] H.-L. Huang, L. Chao, Y.-C. Zhao, L. Wen, X.-M. He, L. Ping, A.-G. Sha, X. Tian, C. J. Papasian, H.-W. Deng, G.-X. Lu, H.-M. Xiao, *Mutant ZP1 in Familial Infertility*, N Engl J Med. **370**(13) (2014), 1220–1226. https://doi.org/10.1056/NEJMoa1308851.

[29] D. Rašković, *Teorija oscilacija (Theory of oscillations) in serbian*, Naučna knjiga, 1965.

[30] A. Hedrih, M. Lazarevic, A. Mitrovic-Jovanovic, *Influence of sperm impact angle on successful fertilization through mZP oscillatory spherical net model*, Comput. Biol. Med. **59**(2015), 19–29. https://doi.org/10.1016/j.compbiomed.2015.01.009.

[31] A. Hedrih, A. Mitrovic-Jovanovic, M. Lazarevic, *Influence of the sperm velocity on fertilization capacity in the oscillatory model of mouse zona pellucida.*, In: Advanced Problems in Mechanics. APM 2019. Lecture Notes in Mechanical Engineering., K.A. Indeitsev, (ed.), 1–21, SpringeSpringer, Cham, 2021. https://doi.org/10.1007/978-3-030-49882-5_1.

[32] A. Hedrih, M. Lazarević, A. Mitrović-Jovanović, *Importance of number of hyperactivated spermatozoa for successful fertilization trough mechanical oscillatory model of mouse Zona Pellucida.*, In: Abstract book of thr 7th Diczfalusy award lecture symposium on reproductive health 27 – 28. Septembar 2013, A. M. Mitrović-Jovanović, (ed.), 27–28, Udruženje za Reproduktivno zdravlje, Megaphone., Belgrade, 2013.

[33] G. F. Clark, *The molecular basis of mouse sperm - Zona pellucida binding: A still unresolved issue in developmental biology*, Reproduction **142**(3) (2011), 377–381. https://doi.org/10.1530/REP-11-0118.

[34] A. Hedrih, M. Lazarevic, A. Mitrovic-Jovanovic, *Influence of sperm impact angle on successful fertilization through mZP oscillatory spherical net model*, Comput. Biol. Med. **59**(2015),. https://doi.org/10.1016/j.compbiomed.2015.01.009.

[35] L. Gómez Montoto, C. Magaña, M. Tourmente, J. Martín-Coello, C. Crespo, J. J. Luque-Larena, M. Gomendio, E. R. S. Roldan, *Sperm competition, sperm numbers and sperm quality in muroid rodents*, PLoS One **6**(3) (2011),. https://doi.org/10.1371/journal.pone.0018173.

[36] Pizzari T, *Of mice and sperm*, PNAS **103**(41) (2006), 14983–14984.

[37] J. M. Bedford, *Why do penetrating sperm create an oblique path in the zona pellucida*, Reproduction **131**(1) (2006), 23–25. https://doi.org/10.1530/rep.1.00901.

[38] A. N. Hedrih, K. R. (Stevanović) Hedrih, *Analysis of energy state of a discrete fractionally damped spherical net of mouse Zona Pellucida before and after fertilization*, Int. J. Mech. Spec. Issue Rab. Fract. Oper. their Some Appl. edsYury A. Ross. Mar. V. Shitikova. **8**(1) (2014), 371–376.

[39] P. Coy and M. Avil´es, *What controls polyspermy in mammals, the oviduct or the oocyte?*, Biol. Rev. **85**(2010), 593–605. https://doi.org/10.1111/j.1469-185X.2009.00117.x.

[40] D. J. Avella MA, Xiong B, *The molecular basis of gamete recognition in mice and humans.*, Mol Hum Reprod. **19**(5) (2013), 279–89. https://doi.org/10.1093/molehr/gat004.

[41] P. Coy, L. Grullon, S. Canovas, R. Romar, C. Matas, M. Aviles, *Hardening of the zona pellucida of unfertilized eggs can reduce polyspermic fertilization in the pig and cow*, Reproduction **135**(1) (2008), 19–27. https://doi.org/10.1530/REP-07-0280.

[42] A. N. Hedrih, M. Lazarević, *Multi-layer oscillatory spherical net model of mouse zona pelucida*, In: Proceedings of 5th International Congress of Serbian Society of Mechanics, Jun15-17th 2015, Arandjelovac, Serbia, Ž. M. Spasić, M. Lazarević, N. Grahovac, (eds.),. p. 8, Published by Serbian Society of Mechanics and Faculty of Technical Sciences Novi Sad, Arandjelovac, 2015.

[43] M. Papi, L. Sylla, T. Parasassi, R. Brunelli, M. Monaci, G. Maulucci, M. Missori, G. Arcovito, F. Ursini, M. De Spirito, *Evidence of elastic to plastic transition in the zona pellucida of oocytes using atomic force spectroscopy*, Appl. Phys. Lett. **94**(15) (2009), 2–5. https://doi.org/10.1063/1.3107265.

[44] Y. Martinova, M. Petrov, M. Mollova, P. Rashev, M. Ivanova, *Ultrastructural study of cat zona pellucida during oocyte maturation and fertilization*, Anim. Reprod. Sci. **108**(3–4) (2008), 425–434. https://doi.org/10.1016/j.anireprosci.2007.09.007.

[45] A. Hedrih, M. Banić, *The effect of friction and impact angle on the spermatozoa-oocyte local contact dynamics*, J. Theor. Biol. **393**(2016), 32–42. https://doi.org/10.1016/j.jtbi.2015.12.031.

[46] M. Papi, A. Maiorana, C. Douet, G. Maulucci, T. Parasassi, R. Brunelli, G. Goudet, M. De Spirito, *Viscous forces are predominant in the zona pellucida mechanical resistance*, Appl. Phys. Lett. **102**(4) (2013), 1–5. https://doi.org/10.1063/1.4789503.

[47] D. M. Woolley, *Motility of spermatozoa at surfaces.*, Reproduction **126**(2003), 259–270.

[48] W. W. Hsiao, H. S. Liao, H. H. Lin, R. F. Ding, K. Y. Huang, C. S. Chang, *Motility Measurement of a Mouse Sperm by Atomic Force Microscopy*, Anal. Sci. **29**(1) (2013), 3–8. https://doi.org/10.2116/ANALSCI.29.3.

[49] S. G. Goodson, Z. Zhang, J. K. Tsuruta, W. Wang, D. A. O'Brien, *Classification of mouse sperm motility patterns using an automated multiclass support vector machines model*, Biol. Reprod. **84**(6) (2011), 1207–1215. https://doi.org/10.1095/biolreprod.110.088989.

[50] A. Hedrih, *Transition in oscillatory behavior in mouse oocyte and mouse embryo trough oscillatory spherical net model of mouse Zona Pellucida*, In: Appl. Non-Linear Dyn. Syst. Springer Proc. Math. Stat., J. Awrejcewicz,ed., Springer International Publishing, 2014, pp. 295–303, 10.1007/978-3-319-08266-0_21. https://doi.org/10.1007/978-3-319-08266-0_21.

[51] V. V. Yashin and A. C. Balazs, *Pattern formation and shape changes in self-oscillating polymer gels*, Science (80-. ). **314**(5800) (2006), 798–801. https://doi.org/10.1126/science.1132412.

[52] A. Hedrih, *Zona pelucida as a mechano-responsive polymer*, In: Abstract book of 24rd International Congress of Theoretical and Applied Mechanics, J. M. Floryan, (ed.), (IUTAM ICTAM Montreal, 2016), 1719–1720, IUTAM, Montreal , Canada, 2016.

[53] A. Hedrih, M. Lazarevic, A. Mitrovic-Jovanovic, *Fertilization as a biomechanical oscillatory phenomenon in mammals*, In: Proceedings of 4th International Congress of Serbian Society of Mechanics, 4-7th June 2013, Vrnjačka Banja, Serbia, N. T., S. Maksimović, T. Igić, (eds.), 579–584, Serbian Society of Mechanics, 2013 (Bograd: Beotele Prom), Vrnjacka Banja, 2013.

[54] A. N. Hedrih, *Transition in oscillatory behavior in mouse oocyte and mouse embryo through oscillatory spherical net model of mouse zona pellucida*, In: Springer Proceedings in Mathematics and Statistics, 2014. https://doi.org/10.1007/978-3-319-08266-0_21.

[55] S. Durán, S. Novo, M. Duch, R. Gómez-Martínez, M. Fernández-Regúlez, A. San Paulo, C. Nogués, J. Esteve, E. Ibañez, J. A. Plaza, *Silicon-nanowire based attachment of silicon chips for mouse embryo labelling*, Lab Chip **15**(6) (2015), 1508–1514. https://doi.org/10.1039/c4lc01299b.

[56] Y. Hara, *Function and Autonomous Behavior of Self-Oscillating Polymer Systems*, Polymers (Basel). **6**(7) (2014), 1958–1971. https://doi.org/10.3390/polym6071958.

[57] V. V. Yashin, K. J. Van Vliet, A. C. Balazs, *Controlling chemical oscillations in heterogeneous Belousov-Zhabotinsky gels via mechanical strain*, Phys. Rev. E - Stat. Nonlinear, Soft Matter Phys. **79**(4) (2009), 79(4 Pt 2):046214. https://doi.org/10.1103/PhysRevE.79.046214.

[58] N. A. Hedrih, J. T. Machado, K. R. (Stevanović) Hedrih, *Electromechanical analogy and generalized function of fractional order energy dissipation in spherical net discrete continuum model of mouse zona pelucida*, In: Proceedings of 5th International Congress of Serbian Society of Mechanics, Jun15-17th 2015, Arandjelovac, Serbia, Ž. M., D. T. Spasić, M. Lazarević, N. Grahovac, (eds.), 1–2, Serbian Society of Mechanics and Faculty of Technical Sciences Novi Sad, Araandjelovac, 2015.

[59] V. V. Yashin, O. Kuksenok, P. Dayal, A. C. Balazs, *Mechano-chemical oscillations and waves in reactive gels*, Reports Prog. Phys. **75**(6) (2012), 066601. https://doi.org/10.1088/0034-4885/75/6/066601.

[60] R. Yoshida, T. Sakai, S. Ito, T. Yamaguchi, *Self-oscillation of polymer chains with rhythmical soluble-insoluble changes*, J. Am. Chem. Soc. **124**(27) (2002), 8095–8098. https://doi.org/10.1021/ja012584q.

[61] A. Hedrih, K. R. (Stevanović) Hedrih, *Multi-parametric dependence of deformationwork of Zona Pelucida in fertilization process trough quasi-static continual shell-like ZP model*, Discontinuity, Nonlinearity, Complex., **6**(4) (2017), 465–476. https://doi.org/10.5890/DNC.2017.12.005.

[62] P. C. Jennings, J. A. Merriman, E. L. Beckett, P. M. Hansbro, K. T. Jones, *Increased zona pellucida thickness and meiotic spindle disruption in oocytes from cigarette smoking mice*, Hum. Reprod. **26**(4) (2011), 878–884. https://doi.org/10.1093/humrep/deq393.

[63] A. N. Hedrih, K. R. (Stevanović) Hedrih, *Deformation work of Zona Pelucida in process of fertilization.*, In: P.O. 13th International Conference on Dynamical Systems – Theory and Applications-DSTA ,December 7-10, 2015, Lodz, Poland, Proceedings-Mechatronics and Life Sciences, J.A. Awrejcewicz, M. Kazmierczak, J. Mrozowski, (eds.), 217–226, Department of Automation, Biomechanics and Mechatronics, Lodz, Lodz, Poland, 2015.

[64] A. Weise, S. Bhatt, K. Piaszinski, N. Kosyakova, X. Fan, A. Altendorf-Hofmann, A. Tanomtong, A. Chaveerach, M. B. De Cioffi, E. De Oliveira, J. U. Walther, T. Liehr, J. P. Chaudhuri, *Chromosomes in a genome-wise order: Evidence for metaphase architecture*, Mol. Cytogenet. **9**(1) (2016), 1–11. https://doi.org/10.1186/s13039-016-0243-y.

[65] A. E. Franklin, W. Z. Cande, *Nuclear organization and chromosome segregation.*, Plant Cell **11**(4) (1999), 523–534.

[66] G. Civelekoglu-Scholey, D. Cimini, *Modelling chromosome dynamics in mitosis: A historical perspective on models of metaphase and anaphase in eukaryotic cells*, Interface Focus **4**(3) (2014),. https://doi.org/10.1098/rsfs.2013.0073.

[67] I. M. Tolić, *Mitotic spindle : kinetochore fibers hold on tight to interpolar bundles*, Eur. Biophys. J. (0123456789) (2017). https://doi.org/10.1007/s00249-017-1244-4.

[68] A. Mogilner, R. Wollman, G. Civelekoglu-Scholey, J. Scholey, *Modeling mitosis*, Trends Cell Biol. **16**(2) (2006), 88–96. https://doi.org/10.1016/j.tcb.2005.12.007.

[69] M. I. Anjur-Dietrich, C. P. Kelleher, D. J. Needleman, *Mechanical Mechanisms of Chromosome Segregation*, Cells **10**(2) (2021),. https://doi.org/10.3390/cells10020465.

[70] J. J. Ward, H. Roque, C. Antony, F. Nédélec, *Mechanical design principles of a mitotic spindle*,(2014), 1–28. https://doi.org/10.7554/eLife.03398.

[71] A. Hedrih, K. R. (Stevanović) Hedrih, *Biomechanical oscillatory model of mitotic spindle*, In: Booklet of abstracts of mini-symposium Biomechanics and modeling of biological systems. December 7, 33–34, Belgrade, 2016.

[72] A. Hedrih, K. R. (Stevanović) Hedrih, *Resonance as potential mechanism for homolog chromosomes separation trough biomechanical oscillatory model of mitotic spindle.*, In: Proceedings of the 6th International Congress of Serbian Society of Mechanics, Mountain Tara, Serbia, June 19-21, M. Lazarevic, et al. , (ed.), 1–10, Serbian Society of Mechanics: Faculty of Mechanical Engineering, University of Belgrade, Belgrade, 2017.

[73] K. R. (Stevanović) Hedrih, *Dynamics of coupled systems*, Nonlinear Anal. Hybrid Syst. **2**(2) (2008), 310–334. https://doi.org/10.1016/J.NAHS.2006.06.003.

[74] Y. Zhao and Q. Zhan, *Electric fields generated by synchronized oscillations of microtubules, centrosomes and chromosomes regulate the dynamics of mitosis and meiosis*, Theor. Biol. Med. Model. **9**(1) (2012), 26. https://doi.org/10.1186/1742-4682-9-26.

[75] J. Lagirand-cantaloube, C. Ciabrini, S. Charrasse, A. Ferrieres, A. Castro, T. Anahory, T. Lorca, *Loss of Centromere Cohesion in Aneuploid Human Oocytes Correlates with Decreased Kinetochore Localization of the Sac Proteins Bub1 and Bubr1*, Nat. Publ. Gr. (February) (2017), 1–14. https://doi.org/10.1038/srep44001.

[76] A. Hedrih, K. R. (Stevanović) Hedrih, *Biomechanical oscillatory model of mitotic spindle*, In: Booklet of abstracts of mini-symposium Biomechanics and modeling of biological systems. December 7, 33–34, Budapest, Hungary, 2016.

[77] K. R. (Stevanović) Hedrih. A. N. Hedrih, *Analysis of oscillatory motions of chromosomes during anaphase using biomechanical oscillatory model of mitotic spindle.*, In: Proceedings of 9th European Nonlinear Dynamics Conference ENOC- 2017, G. C. Gábor Stépán, (ed.),  p. ID 372, CongressLIne Ltd., Budapest, Hungary, 2017.

[78] A. N. Hedrih and K. R. (Stevanović) Hedrih, *Resonant frequencies of mouse chromosomes trough mechanical oscillatory model of mitotic spindle.*, In: ESMC-2018, 10th European Solid Mechanics Conference, July 02.-06. *2018*, p. ID 226, Bolonja, Italy on memory stick, 2018.

[79] A. N. Hedrih, K. R. (Stevanović) Hedrih *Centrosome Frequency Affects Energy of Pairs of Oscillating Chromosomes*, In: The Sixth Conference on Information Theory and Complex Systems TINKOS 2018, June 18-19, 2018, V. Ilic, M. Stankovic, (eds), p.7, Mathematical Institute of the Serbian Academy of Sciences and Arts, Belgrade, Serbia, 2018. https://doi.org/10.22323/1.340.0930.

[80] A. Hedrih, K. R. (Stevanović) Hedrih, *Mitotic Spindle as a Complex Structure: Relation Between Spindle Size and Energy Distribution*, In: The Fifth Conference on Information Theory and Complex Systems TINKOS 2017, November 9-10, 2017, V. Ilic, M. Stankovic, (eds.), p.3, Mathematical Institute SASA, Belgrade, Serbia, Belgrade, Serbia, 2017.

[81] A. N. Hedrih, K. R. (Stevanović) Hedrih, *Potential Energy Analysis of Homologue Chromosome Pairs trough Mechanical Oscillatory Model of Mitotic Spindle*, In: Book of Abstracts of the 11th Chaotic Modeling and Simulation International Conference, C. H. Skiadas, (ed.), p.49, ISAST: International Society for the Advancement of Science and Technology, Rome, Italy, 2018.

[82] A. Hedrih, K. R. (Stevanović) Hedrih, *Kinetic energy of dyads of sister chromatids in a biomechanical oscillatory model of the mitotic spindle*, RAD Conf. Proc. **3** (2019), 225–230. https://doi.org/10.21175/RadProc.2018.47.

[83] N. Sehgal, B. Seifert, H. Ding, Z. Chen, B. Stojkovic, S. Bhattacharya, J. Xu, R. Berezney, *Reorganization of the interchromosomal network during keratinocyte differentiation*, Chromosoma (2016), 389–403. https://doi.org/10.1007/s00412-015-0546-5.

[84] W. A. Bickmore, J. R. Chubb, *Chromosome position: Now, where was I?*, Curr. Biol. **13** (9) (2003), R357–R359. https://doi.org/10.1016/S0960-9822(03)00276-8.

[85] A. Hedrih, K. R. (Stevanović) Hedrih, *Influence of mass chromosome distribution in equatorial plane on oscillatory energy of mitotic spindle trough biomechanical oscillatory model of mitotic spindle*, In: 14th International conference Dynamical Systems - Theory and Applications-DSTA 2017, December 11-14, p.ID: LIF85, Lodz, Poland, 2017.

[86] R. C. Mellors, L. G. Ortega, A. Stoholski, J. Hlinka, *Quantitative cytology and cytopathology. Chromosomal mass in germinal cells and in cancer cells of the mouse*, Exp. Cell Res. **12** (1957), 560–567.

[87] B. Houchmandzadeh, J. F. Marko, D. Chatenay, A. Libchaber, *Elasticity and structure of eukaryote chromosomes studied by micromanipulation and micropipette aspiration*, J. Cell Biol. **139** (1) (1997), 1–12. https://doi.org/10.1083/jcb.139.1.1.

[88] A. Kis, S. Kasas, A. J. Kulik, S. Catsicas, L. Forró, *Temperature-dependent elasticity of microtubules*, Langmuir **24** (12) (2008), 6176–6181. https://doi.org/10.1021/la800438q.

[89] I. V Maly, *Systems Biomechanics of the Cell*, Springer, New York Heidelberg Dordrecht London, 2013. https://doi.org/10.1007/978-1-4614-6883-7.

[90] R. Milo and R. Phillips, *What is the density of cells?*, Cell Biol. by Numbers (2015), 1–5.

[91] J. R. Kuhn, M. Poenie, *Dynamic polarization of the microtubule cytoskeleton during CTL-mediated killing*, Immunity **16** (1) (2002), 111–121. https://doi.org/10.1016/S1074-7613(02)00262-5.

[92] A. Hedrih, K. R. (Stevanović) Hedrih, *Kinetic energy of dyads of sister chromatids in a biomechanical oscillatory model of the mitotic spindle*, In: RAD Conference Proceedings, 2019. https://doi.org/10.21175/RadProc.2018.47.

[93] A. N. Hedrih, K. R. (Stevanović) Hedrih, *Fractional order forced oscillatory modes of elements of the mitotic spindle.*, In: Proceedings of 7th International Congress of Serbian Society of Mechanics, 24-26 June 2019, pp.217–218, M. Lazarević, S. Smić, D. Mađerević, I. Atanasovska, A. Hedrih, & B. Jeremić, (eds.), Sremski Karlovci, Serbia, 2019.

[94] O. A. Goroško, K. R. (Stevanović) Hedrih, *Analitička dinamika diskretnih naslednih sistema, (Analytical Dynamics of Discrete Hereditary Systems)*, University of Niš, Nis, Serbia, 2001.

[95] J. Feser, J. Tyler, *Chromatin structure as a mediator of aging*, FEBS Lett. **585** (13) (2011), 2041–2048. https://doi.org/10.1016/j.febslet.2010.11.016.

[96] M. Ebbinghaus, L. Santen, *Theoretical Modeling of Aging Effects in Microtubule Dynamics*, Biophys. J. (2011), 832–838. https://doi.org/10.1016/j.bpj.2010.11.047.

[97] C. Duellberg, N. I. Cade, T. Surrey, *Microtubule aging probed by microfluidics-Assisted tubulin washout*, Mol. Biol. Cell **27** (22) (2016), 3563–3573. https://doi.org/10.1091/mbc.E16-07-0548.

[98] B. Ibrahim, S. Diekmann, E. Schmitt, P. Dittrich, *In-silico modeling of the Mitotic Spindle Assembly Checkpoint*, PLoS One **3** (2) (2008), 1–11. https://doi.org/10.1371/journal.pone.0001555.

[99] I. V. Maly, *Systems biomechanics of centrosome positioning: A conserved complexity*, Commun. Integr. Biol. **4** (2) (2011), 230–235. https://doi.org/10.4161/cib.4.2.14548.

[100] A. Hedrih, K. R. (Stevanović) Hedrih, *Relation between centrosome excitation and oscillatory energy of mitotic spindle in metaphase trough biomechanical oscillatory model of mitotic spindle*, Invied lecture, In: Mathematics XXI Century & Natural Science, Book of Abstracts, I. Antonov, & W. D. Serow, (eds.), IV International Seminar "Nonlinear Phenomenology Advances (October 3–6, 2017); III International Wokshop, Scientific & Educational Problems of Belarusian Nuclear Power Plant, p.27, St. Petersburg, Publishing House of SPbPU., St. Petersburg, Russia, 2017.